

1   **Effects of spatially heterogeneous lakeside development on nearshore biotic communities in a large,**  
2   **deep, oligotrophic lake (Lake Baikal, Siberia)**

3

4   Michael F. Meyer<sup>1\*</sup>

5   Ted Ozersky<sup>2</sup>

6   Kara H. Woo<sup>3</sup>

7   Kirill Shchapov<sup>2</sup>

8   Aaron W. E. Galloway<sup>4</sup>

9   Julie B. Schram<sup>4</sup>

10   Emma J. Rosi<sup>5</sup>

11   Daniel D. Snow<sup>6</sup>

12   Maxim A. Timofeyev<sup>7</sup>

13   Dmitry Yu. Karnaukhov<sup>7</sup>

14   Matthew R. Brousil<sup>3</sup>

15   Stephanie E. Hampton<sup>3</sup>

16

17   <sup>1</sup>. School of the Environment, Washington State University, Pullman, WA, USA

18   <sup>2</sup>. Large Lakes Observatory, University of Minnesota - Duluth, Duluth, MN, USA

19   <sup>3</sup>. Center for Environmental Research, Education, and Outreach, Washington State University,  
20   Pullman, WA, USA

21   <sup>4</sup>. Oregon Institute of Marine Biology, University of Oregon, Charleston, OR, USA

22   <sup>5</sup>. Cary Institute of Ecosystem Studies, Millbrook, NY, USA

23   <sup>6</sup>. School of Natural Resources, University of Nebraska-Lincoln, Lincoln, NE, USA

24   <sup>7</sup>. Biological Research Institute, Irkutsk State University, Irkutsk, Irkutsk Oblast, Russia

25

26   \*corresponding author: michael.f.meyer@wsu.edu

27

28   **Keywords:** sewage, PPCP, food webs, fatty acids, human disturbance

29

30

31

32   **Abstract (247/250 words)**

33

34   Sewage released from lakeside development can reshape ecological communities. In particular,  
35   nearshore periphyton can rapidly assimilate sewage-associated nutrients leading to increases of  
36   filamentous algal abundance, thus altering both food abundance and quality for grazers. In Lake  
37   Baikal, a large, ultra-oligotrophic, remote lake in Siberia, filamentous algal abundance has  
38   increased near lakeside developments, and localized sewage input is the suspected cause. These  
39   shifts are of particular interest in Lake Baikal, where endemic littoral biodiversity is high,  
40   lakeside settlements are mostly small, tourism is relatively high (~1.2 million visitors annually),  
41   and settlements are separated by large tracts of undisturbed shoreline, enabling investigation of  
42   heterogeneity and gradients of disturbance. We surveyed sites along 40 km of Baikal's  
43   southwestern shore for sewage indicators – pharmaceuticals and personal care products (PPCPs)  
44   and microplastics – as well as periphyton and macroinvertebrate abundance and indicators of  
45   food web structure (stable isotopes and fatty acids). PPCPs, including caffeine and  
46   acetaminophen/paracetamol, were spatially related to lakeside development. As predicted,  
47   lakeside development was associated with more filamentous algae and lower abundance of  
48   sewage-sensitive mollusks. Periphyton and macroinvertebrate stable isotopes and essential fatty  
49   acids suggested that food web structure otherwise remained similar across sites; yet, the  
50   invariance of amphipod fatty acid composition, relative to periphyton, suggested that grazers  
51   adjust behavior or metabolism to compensate for different periphyton assemblages. Our results  
52   demonstrate that even low levels of human disturbance can result in spatial heterogeneity of  
53   nearshore ecological responses, with potential for creating less visible effects that propagate  
54   through the food web.

55

56   **Introduction**

57

58   The release of treated and untreated wastewater into aquatic ecosystems is a common human  
59   disturbance that can introduce pollutants and reshape aquatic ecological communities (Moore et  
60   al. 2003). Nitrogen and phosphorus are among the primary pollutants in wastewater and its  
61   associated byproducts (Smith et al. 1999), yet these nutrients can also originate from disparate  
62   anthropogenic and natural environmental sources, thereby complicating their use as sewage  
63   indicators. For example, agriculture (Powers et al. 2016), watershed processes such as melting  
64   permafrost (Turetsky et al. 2000), and changes in terrestrial plant communities (Moran et al.  
65   2012) can all increase allochthonous nutrient inputs similar to sewage. Regardless of the  
66   nutrients' source, biological processes can further confound sewage detection. Benthic primary  
67   producers, especially those in oligotrophic systems, can assimilate nutrients quickly from the  
68   water column (e.g., hours), such that elevated nutrient concentrations may not be observed  
69   (Hadwen and Bunn 2005).

70

71   Because nutrients come from numerous non-sewage sources, indicators consistently associated  
72   with human activity, such as enhanced  $\delta^{15}\text{N}$  stable isotope signatures (Costanzo et al. 2001;

73 Camilleri and Ozersky 2019), pharmaceuticals and personal care products (PPCPs) (Rosie  
74 Marshall and Royer 2012; Meyer et al. 2019) and microplastics (Barnes et al. 2009), have  
75 garnered increasing attention for their usefulness as sewage indicators. Stable isotopes, such as  
76  $\delta^{15}\text{N}$ , have been frequently used to trace sewage pollution (Gartner et al. 2002), yet their  
77 potential to indicate sewage can be obfuscated by complex terrestrial (Craine et al. 2018) and  
78 aquatic (Guzzo et al. 2011) processes. PPCP studies from continental (Kolpin et al. 2002;  
79 Focazio et al. 2008; Yang et al. 2018) to colloidal pore (Yang et al. 2016) scales, have shown  
80 that PPCP concentrations tend to be greatest closer to their source. In addition to identifying  
81 areas and periods of sewage pollution, PPCPs have also demonstrated robustness in defining  
82 gradients of sewage pollution in river systems, with concentrations being directly proportional to  
83 population density and inversely proportional to distance from a densely populated area (Bendz  
84 et al. 2005). Similar to PPCPs, microplastics (plastic debris up to 5 mm in size) also have been  
85 useful to detect sewage pollution (Li et al. 2018) along gradients of increasing human population  
86 density (Klein et al. 2015), although they can sometimes originate from non-sewage sources,  
87 such as shoreline debris or fishing nets (Free et al. 2014). In contrast to  $\delta^{15}\text{N}$  signatures and  
88 PPCPs concentrations, microplastics are typically resistant to degradation (Barnes et al. 2009),  
89 providing a signal over a longer time frame than many PPCPs and nutrients in sewage. As a  
90 result of each pollutant's consistent association with sewage, co-located  $\delta^{15}\text{N}$ , PPCP, and  
91 microplastic measurements can be used to infer the spatial extent and timing of sewage pollution  
92 in an ecosystem.

93  
94 The effects of sewage pollution are frequently first seen in nearshore benthic communities where  
95 increased nutrients alter algal species composition, abundance, nutritional quality, as well as  
96 food web trophic structure. Increased filamentous algal abundance, for example, has been  
97 frequently observed in areas suspected of sewage pollution (Rosenberger et al. 2008; Hampton et  
98 al. 2011), likely due to benthic filamentous algae efficiently removing nutrients from the water  
99 column (Hadwen and Bunn 2005; Andersson and Brunberg 2006). With a changing resource  
100 base, grazing macroinvertebrate communities may likewise shift to include more detritivores or  
101 species capable of consuming filamentous algae (Rosenberger et al. 2008). In addition to some  
102 grazers' physical difficulty consuming filamentous algae (Mazzella and Russo 1989), there also  
103 may be changes in algal nutritional quality, as filamentous algae tend to contain a different  
104 mixture of essential fatty acids (EFAs) in comparison to diatoms (Kelly and Scheibling 2012),  
105 which dominate periphyton communities in unimpacted ecosystems. In particular, the EFAs  
106 18:3 $\omega$ 3 and 18:2 $\omega$ 6 are commonly associated with green filamentous algae (Taipale et al. 2013),  
107 whereas 20:5 $\omega$ 3 is more associated with diatoms (Taipale et al. 2013). All EFAs are largely  
108 synthesized by primary producers, and each related group produces strongly differentiated  
109 multivariate signatures (Taipale et al. 2013; Galloway and Winder 2015). Consumers can acquire  
110 fatty acids by grazing (Dalsgaard et al. 2003) or upgrading fatty acids at their own energetic  
111 expense (Sargent and Falk-Petersen 1988; Dalsgaard et al. 2003) and often reflect the fatty acid

112 signatures of their diets. Thus, comparing consumer and producer fatty acid compositions can be  
113 used to infer how grazing patterns change in response to increasing sewage pollution.

114  
115 To investigate lake littoral community and food web responses to sewage pollution, we surveyed  
116 40 km of Lake Baikal's shoreline for indicators of sewage pollution and metrics of benthic  
117 community composition and structure. Located in Siberia, Lake Baikal is the oldest, most  
118 voluminous, and deepest freshwater lake in the world (Hampton et al. 2018), with the majority of  
119 Lake Baikal's biodiversity occurring in the littoral zone (Kozhova and Izmest'eva 1998). While  
120 Lake Baikal's pelagic zone is generally ultra-oligotrophic (Yoshida et al. 2003; O'Donnell et al.  
121 2017), nearshore areas abutting lakeside settlements have shown distinct signs of eutrophication  
122 (Timoshkin et al. 2016). Much of Lake Baikal's shoreline lacks human development and  
123 Baikal's watershed is largely roadless and unpopulated (Moore et al. 2009). Despite low levels of  
124 development, uncharacteristic filamentous algal blooms have been occurring throughout the lake  
125 since 2010 (Kravtsova et al. 2014; Timoshkin et al. 2016; Volkova et al. 2018). While increased  
126 *Ulothrix* spp. abundance historically occurs in late summer (Kozhov 1963; Kozhova and  
127 Izmest'eva 1998), recent observations of *Spirogyra* spp. abundance at unprecedented levels are  
128 thought to be associated with increased nearshore nutrient concentrations (Volkova et al. 2018;  
129 Ozersky et al. 2018). Inadequate wastewater management in lakeside settlements is likely the  
130 main driver of these nearshore algal blooms (Timoshkin et al. 2016, 2018), motivating further  
131 research to identify the extent to which sewage is altering nearshore communities

132  
133 Given the growing evidence that Baikal's nearshore periphyton communities are responding to  
134 sewage inputs, our goal was to understand how littoral benthic community composition and  
135 interactions may be changing near areas of sewage pollution. This overarching goal was divided  
136 into three specific objectives:

- 137 1. identify areas of wastewater pollution using consistent sewage indicators,
- 138 2. assess the relationship between sewage indicators and littoral periphyton and  
139 macroinvertebrate community composition, and
- 140 3. evaluate how food webs may restructure with increasing sewage pollution.

141 We hypothesized that (1) sewage indicators, such as PPCP concentrations,  $\delta^{15}\text{N}$ , and  
142 microplastic densities, would increase with increasing population density and proximity of  
143 lakeside development; (2) an increasing sewage signal would correlate with increased dominance  
144 of filamentous benthic algae; and (3) increasing filamentous algae abundance would result in  
145 changes in the abundance of different macroinvertebrate feeding guilds, reflected in community  
146 composition and dietary tracers such as carbon and nitrogen stable isotopes and fatty acids.

147

## 148 **Methods**

149

### 150 *I. Site description*

151

152 The vast majority of Lake Baikal's 2,100-km shoreline lacks lakeside development (Moore et al.  
153 2009; Timoshkin et al. 2016). Our study focused on a 40-km section of Baikal's southwestern  
154 shoreline, which included three settlements of different sizes (Figure 1; Figure 2). From 19  
155 through 23 August 2015, we sampled 14 littoral and 3 pelagic locations along our 40-km  
156 transect. Littoral locations were chosen to capture a range of sites with varying degrees of  
157 adjacent shoreline development – from “developed” (along the waterfront of human settlements)  
158 to “undeveloped” (no adjacent human settlements and complete forest cover; Figure 1; Figure 2;  
159 Table 1). Pelagic sites were located 2 to 5 km offshore from each of the developed sites in water  
160 depths of 900-1300 m (Figure 1; Table 1). All littoral sites were sampled at approximately the  
161 same depth (~1.25 m) at a distance of 8.90-20.75 m from shore (Table 1). At each site, air  
162 temperature was measured with a mercury thermometer, and photographs were taken of the  
163 substrate and the shoreline.

164

165 Three discrete lakeside settlements were located along our 40-km transect. The largest,  
166 Listvyanka, is primarily a tourist town of approximately 2000 permanent residents, although  
167 tourism can contribute significantly to the town's population with approximately 1.2 million  
168 annual visitors (Interfax-Tourism 2018). The other two settlements are the villages Bolshie Koty  
169 and Bolshoe Goloustnoe, which have approximately 80 and 600 permanent residents,  
170 respectively. Bolshie Koty is home to two field research stations and several small tourist  
171 accommodations. Bolshoe Goloustnoe has several hotels and tourist camps. Although Bolshie  
172 Koty and Bolshoe Goloustnoe are built along small streams that empty into Baikal, there are no  
173 upstream developed sites, meaning that any observed sewage indicators in Baikal most likely  
174 originated either from Bolshie Koty or Bolshoe Goloustnoe.

175

#### 176 *Inverse distance weighted (IDW) population calculation*

177

178 We recognized that sewage indicator concentrations at each sampling location may be related to  
179 a sampling location's spatial position relative to both the size and proximity of neighboring  
180 developed sites. Therefore, we created the inverse distance weighted (IDW) population metric to  
181 compress, into a single metric, information about human population size, density, and location  
182 along the shoreline as well as distance between developed sites and sampling locations. The  
183 IDW metric reflects the idea that sewage pollution should be positively related to increasing  
184 human density and inversely related with distance from densely populated areas (*sensu* Bendz et  
185 al., 2005). Additionally, Timoshkin et al. (2018) noted that sewage enters Baikal's nearshore  
186 largely through groundwater, implying that locations with more directly adjacent shoreline  
187 development should experience higher sewage concentrations in the lake. Acknowledging that  
188 nearshore PPCP concentrations were likely positively proportional to a developed location's  
189 shoreline length, we scaled a developed site's population density by its shoreline length. This  
190 scaling represents population density that directly interfaces with the lake, thereby capturing the  
191 idea that sewage-associated pollutants, such as PPCPs (Karnjanapiboonwong et al. 2010) and

192 nutrients (de Vries 1972), contributed away from the shoreline can be removed via the soil  
193 matrix en route to the lake.

194

195 Our calculation of IDW population was done in five steps. First, we traced polygons and  
196 shorelines from satellite imagery for each developed site in Google Earth. Polygons were traced  
197 for the entire area of visible development (Figure 2). Similarly, shoreline traces only reflected  
198 shoreline length for which there was visible development (Figure 2). Second, polygon and line  
199 geometries were downloaded from Google Earth as a .kml file. Third, the .kml file was imported  
200 into the R statistical environment (R Core Team 2019) where, using the sf package (Pebesma,  
201 2018), we calculated shoreline length, polygon area, and centroid location for each developed  
202 site. Fourth, we joined point locations of each sampling site with the spatial polygons to calculate  
203 the distance from each sampling location to each developed site's centroid. Fifth, we calculated  
204 IDW population for each sampling location, using formula (1)

205 (1)  $I_j = \frac{P_{LI} * L_{LI}}{A_{LI}} + \frac{P_{BK} * L_{BK}}{A_{BK}} + \frac{P_{BGO} * L_{BGO}}{A_{BGO}}$

206 where  $I$  is the IDW population at sampling location  $j$ ,  $P$  is the population at each of the three  
207 developed sites Listvyanka (LI), Bolshie Koty (BK), Bolshoe Goloustnoe (BGO),  $A$  is the area of  
208 a developed site in  $\text{km}^2$ ,  $L$  is the shoreline length at a developed site in km, and  $D$  is the distance  
209 from sampling site  $j$  to each developed site's centroid in km. This formulation implies that all  
210 sampling locations are influenced by all three developed sites. Thus, the influence of an  
211 individual developed site on each sampling location is positively influenced by the numerical  
212 and spatial density of the population and its orientation toward the shoreline, and inversely  
213 proportional to a sampling location's distance from each of the three developed sites.

214

## 215 *2. Water samples*

216

217 At both pelagic and littoral sites, water samples were collected for nutrient, chlorophyll,  
218 microplastic, and PPCP analysis. Samples were collected by hand from 0.75 m depth for each  
219 littoral site and with a bucket from aboard the Irkutsk State University “Kozhov” research vessel  
220 for pelagic sites. Each water sample collection procedure is described below.

221

### 222 *2a. Nutrients*

223

224 Water samples for nutrient analyses were collected in 150 mL glass jars that had been washed  
225 with phosphate-free soap and rinsed three times with water from the sampling location. Samples  
226 were collected in duplicates and immediately frozen at -20°C until processing at the A.P.  
227 Vinogradov Institute of Geochemistry (Siberian Branch of the Russian Academy of Sciences,  
228 Irkutsk). Samples were not filtered prior to freezing, meaning that nitrogen and ammonium  
229 concentrations may potentially include intracellular nitrogen and overestimate nitrogenous forms  
230 in the water column.

231  
232 For each water sample, nitrate, ammonium, and total phosphorus concentrations were measured.  
233 For ammonium (2016a) and nitrate (2017) concentrations, samples were analyzed with a  
234 spectrophotometer following the addition of Nessler's reagent and disulfuric acid respectively.  
235 Total phosphorus concentration was measured with a spectrophotometer following the addition  
236 of persulfate (2016b). Concentrations are reported in mg/L.

237

238 *2b. Chlorophyll a*

239  
240 Water samples were collected in 1.5 L plastic bottles from a depth of approximately 0.75 m.  
241 Within 12 h of collection, three subsamples (up to 150 mL each) were filtered through 25-mm  
242 diameter, 0.2 µm pore size nitrocellulose filters. Filters were then placed in a 35-mm petri dish  
243 and frozen in the dark until processing.

244

245 Chlorophyll samples were processed in a manner similar to that of Parsons and Strickland (1963)  
246 and Lorenzen (1967). Nitrocellulose filters were ground in 90% acetone, in which chlorophyll  
247 extraction was allowed to proceed overnight. Samples were then centrifuged for 15-20 minutes.  
248 After centrifugation, absorbance of the chlorophyll extract was measured in a spectrophotometer  
249 at 630, 645, 665, and 750 nm. Concentrations were calculated using the formula:  $C =$   
250  $11.64(A_{665} - A_{750}) - 2.16(A_{645} - A_{750}) - 0.1(A_{630} - A_{750}) / (V_2/V_1)$ ; where A is the  
251 absorbance value of a particular wavelength, V<sub>1</sub> is the volume of the filtered water, and V<sub>2</sub> is the  
252 volume of extract. Concentrations are reported as mg/L.

253

254 *2c. PPCPs*

255  
256 Water samples for PPCP analysis were collected in 250 mL amber glass bottles that were rinsed  
257 with either methanol or acetone and then three times with sample water prior to collections.  
258 Following collection, samples were refrigerated and kept in the dark until solid phase extraction  
259 (SPE).

260

261 Within 12 h of collection, samples were filtered directly from the amber glass bottle using an in-  
262 line Teflon filter holder with glass microfiber GMF (1.0 µm pore size, WhatmanGrad 934-AH)  
263 in tandem with a solid phase extraction (SPE) cartridge (200 mg HLB, Waters Corporation,  
264 Milford, MA) connected to a 1-liter vacuum flask. Lab personnel wore gloves and face masks to  
265 minimize contamination. Prior to filtration, SPE cartridges were primed with at least 5 mL of  
266 either methanol or acetone and then washed with at least 5 mL of sample water. Rate of  
267 extraction was maintained at approximately 1 drop per second. Extraction proceeded until water  
268 could no longer pass through the SPE cartridge or until all collected water was filtered.  
269 Cartridges were stored in Whirlpacks at -20°C until analysis for 18 PPCP residues using liquid

270 chromatography tandem mass spectrometry (LC-MS-MS) following methods of Lee et al. (2016)  
271 and D'Alessio et al (2018). Concentrations are reported in µg/L.

272

273 *2d. Microplastics*

274

275 At each location, samples were collected in triplicate using 1.5 L clear plastic bottles that were  
276 washed thoroughly with sample water before each collection. Samples were collected by hand  
277 for each littoral site and with a metal bucket from aboard the ship for pelagic sites.

278

279 For processing, each sample was vacuum filtered on to a 47-mm diameter GF/F filter. During  
280 filtration, aluminum foil was used to cover the filtration funnel to prevent contamination from  
281 airborne microplastic particles. After filtration, filters were dried under vacuum pressure and  
282 then stored in 50-mm petri dishes. Following filtration of all three replicates, the filtrate was  
283 collected and then re-filtered through a GF/F filter as a control for contamination from the plastic  
284 vacuum funnel or potentially airborne microplastics.

285

286 Microplastic counting involved visual inspection of the entire GF/F in a similar manner to  
287 methods described in Hanvey et al. (2017). Visual enumeration was conducted under a stereo  
288 microscope with ~100x magnification, and microplastics were classified into one of three  
289 categories: fibers, fragments, or beads. For all categories, plastics were defined as observed  
290 objects with apparent artificial colors, so as to not enumerate plastics potentially contributed  
291 from the sampling bottle itself. Fibers were defined as smooth, long plastics with consistent  
292 diameters. Fragments were defined as plastics with irregularly sharp or jagged edges. Beads were  
293 defined as spherical plastics. Although we did not measure microplastic size, this technique  
294 likely allowed us to reliably quantify microplastics as small as ~300 µm (Hanvey et al. 2017).  
295 During enumeration, GF/Fs remained covered in the petri dish to minimize potential for  
296 contamination from the air. Following enumeration of both experimental and control samples,  
297 fibers, fragments, and beads enumerated in the controls were subtracted from the experimental  
298 microplastic densities for each plastic type and from each replicate. One location (BK-1) had two  
299 control replicates, which were averaged for each plastic type and then subtracted from the  
300 experimental samples. Results are reported as the average number of microplastics/L.

301

302 *3. Benthic biological samples*

303

304 At each littoral site, periphyton and macroinvertebrates were collected for relative abundance  
305 estimates and food web analysis by wading and snorkeling.

306

307 *3a. Benthic algal collection*

308

309 At each littoral site, we haphazardly selected three rocks representative of local substrate. A  
310 plastic stencil was used to define a surface area of each rock from which we scraped a  
311 standardized 14.5 cm<sup>2</sup> patch of periphyton. Samples were preserved with Lugol's solution and  
312 stored in plastic scintillation vials. Additional periphyton was collected in composite from each  
313 site for fatty acid and stable isotope analysis.

314

315 Periphyton taxonomic identification and enumeration was performed by subsampling 10 µL  
316 aliquots from each preserved sample. For all 10 µL aliquots, cells, filaments, and colonies were  
317 counted, for the entire subsample, until at least 300 cells were identified for a given sampling  
318 replicate. When the first aliquot contained less than 300 cells, we counted additional subsamples  
319 until we reached at least 300 cells in total. In instances when 300 cells were counted before  
320 finishing a subsample, we still counted the entire aliquot. Taxa were classified into broad  
321 categories consistent with Baikal algal taxonomy (Izhboldina 2007), using coarse groupings to  
322 capture general patterns in relative algal abundance. As a result, algal groups consisted of  
323 diatoms, *Ulothrix*, *Spirogyra*, and the green algal Order Tetrasporales.

324

### 325 *3b. Benthic invertebrate collection*

326

327 At each littoral site, three kick-net samples were collected for assessment of benthic community  
328 composition and abundance. Using a D-net, we collected macroinvertebrates by flipping over 1-3  
329 rocks, and then sweeping five times in a left-to-right motion across approximately 1 m. After the  
330 series of sweeps, the catch was rinsed into a plastic bucket. For each replicate, bucket contents  
331 were concentrated using a 64-µm mesh and placed in glass jars with 40% ethanol (vodka; the  
332 only preservative available to us at the time) for preservation and refrigerated at 4°C aboard the  
333 research vessel. The 40% ethanol preservative was replaced with ~80% ethanol upon return to  
334 the lab within 24 to 48 hours, and samples were stored at ~4°C.

335

336 Separate collections were conducted for invertebrate fatty acid and stable isotope analyses.  
337 Invertebrates were collected using a D-net in a similar fashion as the community enumeration.  
338 Additional invertebrates were also collected by hand. Collected organisms were then live-sorted,  
339 identified to species, and frozen at -20°C at the field station. The samples were later transferred  
340 to the lab in the US via a Dewar flask with dry ice.

341

342 Invertebrate taxonomic identification and enumeration were performed under a stereo  
343 microscope. All invertebrates were identified to species with the exception of juveniles  
344 (Takhteev and Didorenko (2015) for amphipods; Sitnikova (2012) for mollusks; Table 2). All  
345 samples contained oligochaetes and polychaetes, but due to poor preservation, these taxa were  
346 not counted. Six samples of the 42 collected were not well-preserved and were excluded from  
347 further analyses, in order to reduce errors in identification. KD-1 and LI-1 were the only sites  
348 with 1 sample counted. BK-2 and KD-2 each had two samples counted.

349

350 *3c. Food web characterization*

351

352 To characterize littoral food webs, we analyzed carbon and nitrogen stable isotopes as well as  
353 fatty acid profiles for periphyton and macroinvertebrates. Prior to isotopic and fatty acid  
354 analysis, periphyton and macroinvertebrate samples were lyophilized for ~24 hours,  
355 homogenized to powder, and then weighed.

356

357 *Stable isotope analysis*

358

359 Measurements of  $\delta^{15}\text{N}$  and  $\delta^{13}\text{C}$  were performed on an elemental analyzer-isotope ratio mass  
360 spectrometer (EA-IRMS; Finnigan DELTAplus XP, Thermo Scientific) at the Large Lakes  
361 Observatory, University of Minnesota Duluth. The EA-IRMS was calibrated against certified  
362 reference materials including L-glutamic acid (NIST SRM 8574), low organic soil and sorghum  
363 flour (standards B-2153 and B-2159 from Elemental Micro-analysis Ltd., Okehampton, UK) and  
364 in-house standards (acetanilide and caffeine). Replicate analyses of external standards showed a  
365 mean standard deviation of 0.06 ‰ and 0.09 ‰, for  $\delta^{13}\text{C}$  and  $\delta^{15}\text{N}$ , respectively.

366

367 *Fatty acid analysis*

368

369 Following freeze-drying, samples were transferred to 10 mL glass centrifuge vials, and 2 mL of  
370 100% chloroform was added to each under nitrogen gas. Samples remained in chloroform  
371 overnight at -80°C. Fatty acid extractions generally involved three phases: (1) 100% chloroform  
372 extraction, (2) chloroform-methanol extraction, and (3) fatty acid methylation. Fatty acid  
373 extraction methods were adapted from Schram et al. (2018).

374

375 After overnight chloroform extraction, samples underwent a chloroform-methanol extraction  
376 three times. To each sample, we added 1 mL cooled 100% methanol, 1 mL chloroform:methanol  
377 solution (2:1), and 0.8 mL 0.9% NaCl solution. Samples were inverted three times and sonicated  
378 on ice for 10 minutes. Next, samples were vortexed for 1 minute, and centrifuged for 5 minutes  
379 (3,000 rpm) at 4°C. Using a double pipette technique, the lower organic layer was removed and  
380 kept under nitrogen. After the third extraction, samples were evaporated under nitrogen flow, and  
381 resuspended in 1.5 mL chloroform and stored at -20°C overnight.

382

383 Once resuspended in chloroform, 1 mL of chloroform extract was transferred to a glass  
384 centrifuge tube with a glass syringe as well as an internal standard of 4 µL of 19-carbon fatty  
385 acid. Samples were then evaporated under nitrogen, and then 1 mL of toluene and 2 mL of 1%  
386 sulfuric acid-methanol was added. The vial was closed under nitrogen gas and then incubated in  
387 50°C water bath for 16 hours. After incubation, samples were removed from the bath, allowed to  
388 reach room temperature and stored on ice. Next, we performed a potassium carbonate-hexane  
389 extraction twice. To each sample, we added 2 mL of 2% potassium bicarbonate and 5 mL of

390 100% hexane, inverting the capped vial so as to mix the solution. Samples were centrifuged for 3  
391 minutes (1,500 rpm) at 4°C. The upper hexane layer was then removed and placed in a vial to  
392 evaporate under nitrogen flow. Once almost evaporated, 1 mL of 100% hexane was added and  
393 stored in a glass amber autosampler vial for GC/MS quantification. GC/MS quantification was  
394 performed with a Shimadzu QP2020 GC/MS following Schram et al. (2018).

395

396 *4. Statistical analyses*

397

398 Total phosphorus, nitrate, ammonium, microplastic abundance and density, total PPCP  
399 concentration, and  $\delta^{15}\text{N}$  values in macroinvertebrate tissues were log-transformed and regressed  
400 against log-transformed IDW population using a linear model. Analytically, log-transforming  
401 made sites comparable, as values spanned three orders of magnitude. Physically, we assumed  
402 that sewage indicators were likely subject to exponential processes (e.g., mixing, diffusion), and  
403 log-transforming the data should linearize the relationships between predictor and response  
404 variables. Residuals were assessed for normality and homogeneity of variance.

405

406 To assess if benthic community composition was associated with increasing sewage indicators,  
407 periphyton and macroinvertebrate abundance data were each analyzed with a consistent  
408 multivariate workflow. First, replicates were averaged, and taxonomic groups representing less  
409 than 1% of the inter-site community were removed from analysis, in order to reduce the  
410 influence of rare species on results. Second, community compositions for both periphyton and  
411 macroinvertebrates were visualized using non-metric multidimensional scaling (NMDS) with a  
412 Bray-Curtis similarity metric. Periphyton community compositions were calculated as relative  
413 proportions, whereas invertebrate abundances were grouped at the genus-level and then square-  
414 root transformed to minimize influence of more abundant taxa. Visual inspection of the NMDS  
415 plot suggested that sites generally tended to separate by increasing PPCP concentrations and  
416 IDW population (see Table 2). To test whether sites' benthic communities significantly differed  
417 with increasing PPCP concentration and IDW population, we first used k-mediods, also known  
418 as Partitioning Around the Mediods (PAM; Kaufman and Rousseeuw 2005), clustering to  
419 identify an optimal number of groupings (Figure S1). For this process, we iterated through  
420 multiple numbers of clusters (i.e., 1 to 10) and calculated the within-group-sum-of-squares (wss)  
421 and average silhouette width. We identified the optimal number of groups when wss decreased  
422 most markedly and when silhouette width was greatest (i.e., the elbow method) (Johnson and  
423 Wichern 2007). To confirm the optimal number as determined by non-hierarchical PAM  
424 clustering, we also used Weighted Pair-Group Centroid Clustering (WPGMC) as a hierarchical  
425 approach (Sneath and Sokal 1973), which corrects for clusters that may not be strongly  
426 discriminated regardless of how many samples are assigned to a given cluster (Legendre and  
427 Legendre 2012). We then performed two permutational multivariate analyses of variance  
428 (PERMANOVA; Anderson 2001) with 999 permutations: the first where community  
429 compositions were responses to the groups identified through clustering and the second where

430 community compositions were responses to the continuous IDW population. Unlike traditional  
431 multivariate analyses of variance (MANOVA), PERMANOVA does not require assumptions of  
432 multivariate normality (Anderson 2001). When significant differences were identified, post-hoc  
433 SIMPER analysis (Clarke 1993) was performed following the PERMANOVA to identify which  
434 taxonomic groups contributed to 85% of the cumulative variance that most influenced site  
435 separation.

436

437 To assess whether benthic food webs restructured with increasing sewage indicator  
438 concentrations, fatty acid data were analyzed in a manner similar to periphyton and  
439 macroinvertebrate abundance data. First, species' fatty acid profiles were visualized by  
440 performing NMDS with Bray-Curtis similarity for all organisms' relative fatty acid abundance  
441 (Figure S2). This technique broadly demonstrated that, as expected, interspecific variation in  
442 fatty acid composition was greater than intraspecific variation. The same pattern was observed  
443 for all fatty acids quantified as well as solely essential fatty acids (EFAs; Figure S2). Together,  
444 these NMDS plots suggested that periphyton fatty acids at sites differentiated based on sewage  
445 indicator concentrations, which was likely a reflection of differences in periphyton community  
446 composition (Taipale et al. 2013). Among all taxa and sites, 18:3 $\omega$ 3, 18:1 $\omega$ 9, and 20:5 $\omega$ 3 had the  
447 highest coefficients of variation, enabling comparisons between sites. These fatty acids tend to  
448 be associated with filamentous green algae (i.e., 18:3 $\omega$ 3 and 18:1 $\omega$ 9) and diatoms (i.e., 20:5 $\omega$ 3).  
449 To increase the robustness of our analysis, we expanded our approach to include major fatty  
450 acids within each taxonomic group, including 18:2 $\omega$ 6 (abundant in green algae); 16:1 $\omega$ 7 and  
451 14:0 (abundant in diatoms); and 16:0 (abundant in both green algae and diatoms) (Taipale et al.  
452 2013). To evaluate how relative fatty acid abundance may relate to sewage pollution, we  
453 assessed patterns among these seven fatty acids with both multivariate and univariate  
454 approaches. Within a multivariate framework, we created two NMDS plots with Bray-Curtis  
455 similarity, one just with primary producer (Figure S5) and the other with macroinvertebrate  
456 (Figure S6) fatty acid profiles. Because multivariate patterns suggested fatty acid profiles may  
457 relate to sewage pollution, we regressed a filamentous:diatom fatty acid signal ratio (Equation 2)

$$458 (2) \frac{18:3\omega 3\% + 18:1\omega 9\% + 18:2\omega 6\% + 16:0\%}{20:5\omega 3\% + 16:1\omega 7\% + 16:0\% + 14:0\%}$$

459 against log-transformed PPCP concentrations using a linear model. Additionally, we evaluated  
460 how three essential fatty acids (18:3 $\omega$ 3, 18:2 $\omega$ 6, and 20:5 $\omega$ 3), lipids thought to accumulate in  
461 biological systems, may differ in abundance across the sewage gradient. Therefore, we similarly  
462 regressed the ratio of  $\frac{18:3\omega 3\% + 18:2\omega 6\%}{20:5\omega 3\%}$  against log-transformed PPCP concentrations using a  
463 linear model.

464

465 All analyses were conducted in the R statistical environment (R Core Team 2019), using the  
466 tidyverse (Wickham et al. 2019), factoextra (Kassambara and Mundt 2019), cluster (Maechler et  
467 al. 2019), pvclust (Suzuki et al. 2019), ggrepel (Slowikowski 2019), viridis (Garnier 2018), fs  
468 (Hester and Wickham 2019), spdplyr (Sumner 2019), janitor (Firke 2020), sf (Pebesma 2018),  
469 ggpubr (Kassambara 2019), ggtext (Wilke 2020), OpenStreetMap (Fellows and Stotz 2019),

470 cowplot (Wilke 2019), and vegan (Oksanen et al. 2019) packages. All data, including .kml files  
471 used to calculate IDW metric, are publicly available from the Environmental Data Initiative  
472 repository (Meyer et al. 2020), and all R scripts are available from the GitHub repository of this  
473 project's Open Science Framework account (Meyer et al. 2015).

474

## 475 Results

476

### 477 1. Water samples

478

479 Nearshore water nitrate ( $R^2 = 0.01$ ,  $p = 0.68$ ), ammonium ( $R^2 = 0.17$ ,  $p = 0.11$ ), total phosphorus  
480 ( $R^2 = 0.14$ ,  $p = 0.14$ ), and chlorophyll a ( $R^2 = 0.11$ ,  $p = 0.20$ ) concentrations were not  
481 significantly correlated with IDW population (Figure 3). Total PPCP ( $R^2 = 0.26$ ,  $p = 0.04$ )  
482 concentrations were significantly related with IDW population (Figure 3). In the littoral zone,  
483 PPCPs detected included caffeine, 1,7-dimethylxanthine/paraxanthine (main human metabolite  
484 of caffeine), cotinine (main human metabolite of nicotine), and acetaminophen/paracetamol  
485 (Table 3). Other PPCPs, including carbamazepine, diphenhydramine, thiabendazole,  
486 amphetamine, methamphetamine, MDA, MDMA, morphine, phenazone, sulfachloropyridazine,  
487 sulfamethazine, sulfadimethoxine, sulfamethazole, trimethoprim, and cimetidine, were not  
488 detected.

489

490 Microplastics were detected in samples from both littoral and pelagic sites. Bead microplastics  
491 were only detected near Listvyanka. Fibers (mean = 0.85 microplastics/L, std dev = 1.21  
492 microplastics/L) and fragments (mean = 0.83 microplastics/L, std dev = 1.35 microplastics/L)  
493 were the most abundant types of microplastics across all sites, whereas beads were relatively rare  
494 (mean = 0.08 microplastics/L, std dev = 0.31 microplastics/L). Total microplastic densities were  
495 not significantly correlated with IDW population ( $R^2 = 0.01$ ,  $p = 0.65$ ; Figure 3), although more  
496 types of microplastics were generally observed near areas with higher IDW population values,  
497 such as Listvyanka.

498

### 499 2. Benthic biological samples

500

#### 501 2a. Periphyton

502

503 Major taxonomic groupings of periphyton consisted of diatoms, *Tetrasporales* spp., *Spirogyra*  
504 spp., and *Ulothrix* spp. K-medoids (Figures S1a; S2a) and WPGMC (Figure S3a) cluster  
505 analyses of periphyton abundance demonstrated two groupings capture most variance, and visual  
506 inspection of relative periphyton community abundance NMDS suggested groupings were  
507 related to IDW population values (Figure 4). PERMANOVA results demonstrated that  
508 periphyton communities were significantly different based on IDW population groupings ( $R^2 =$   
509 0.52,  $p = 0.001$ ) and the continuous IDW population ( $R^2 = 0.43$ ,  $p = 0.001$ ). Post-hoc SIMPER

510 results suggested that these differences were primarily associated with sites that had higher  
511 *Ulothrix* spp. and *Spirogyra* spp. relative abundance. Additionally, sites with high IDW  
512 populations had lower diatom relative abundance in comparison to sites with low and moderate  
513 IDW populations.

514

### 515 2b. Macroinvertebrates

516

517 Taxonomic groupings included five amphipod genera: *Eulimnogammarus*, *Poekilogammarus*,  
518 *Cryptoropus*, *Brandtia* and *Pallasea*; six mollusk families: Planorbidae, Valvatidae, Baicaliidae,  
519 Benedictidae, Acroloxidae, Maackia; flatworms; caddisflies; and leeches (summarized in Table  
520 S1). K-mediod cluster analysis of macroinvertebrate community composition suggested 2 or 3  
521 major groupings would capture most variance (Figure S1b; S2b), whereas WPGMC analyses  
522 suggested 2 groupings would enable all sites except for one to be assigned a cluster (S3b).  
523 Because both forms of hierarchical and non-hierarchical clustering suggested two groupings as  
524 optimal, we proceeded using two groupings. Visual inspection of NMDS suggested clusters were  
525 related to IDW population (Figure 5). PERMANOVA results supported the hypothesis that  
526 macroinvertebrate communities significantly differed both among our IDW population groupings  
527 ( $R^2 = 0.19$ ,  $p = 0.02$ ) and along our continuous gradient of increasing IDW population ( $R^2 =$   
528  $0.19$ ,  $p = 0.02$ ). Post-hoc SIMPER analyses suggested that *Poekilogammarus*,  
529 *Eulimnogammarus*, Valvatidae, Caddisflies, *Brandtia*, Baicaliidae, Planorbidae, *Cryptoropus*,  
530 and flatworms contributed the greatest differences between high and moderate/low IDW  
531 population groupings (see Table 2).

532

### 533 3. Food web characterization: stable isotopes and fatty acids

534

535 Among periphyton and amphipod samples,  $\delta^{13}\text{C}$  values ranged from -19.5 to -9.5 ‰ (Figure 6).

536 Among periphyton samples,  $\delta^{15}\text{N}$  values ranged from 0.77 to 3.76 ‰, whereas amphipod  $\delta^{15}\text{N}$   
537 values ranged from 6.42 to 7.92 ‰.

538

539 For grazers,  $\delta^{15}\text{N}$  significantly increased with IDW population ( $p = 0.01$ ; Figure 3, Figure 6).

540 Periphyton  $\delta^{15}\text{N}$  signatures did not significantly increase with IDW population ( $p = 0.27$ ). In  
541 contrast,  $\delta^{13}\text{C}$  concentrations were not related with IDW population for either periphyton or  
542 macroinvertebrates.

543

544 With respect to fatty acids, macroinvertebrates tended to be characterized by mono-unsaturated  
545 fatty acids (MUFAAs) and long-chain (i.e.  $\geq 20$ -Carbons) polyunsaturated fatty acids (LCPUFAs),  
546 whereas periphyton tended to be characterized by short-chain (i.e., 16- and 18-Carbons)  
547 polyunsaturated fatty acids (SCPUFAs) (Table 3). When comparing proportions within taxa  
548 across the sewage gradient, periphyton SCPUFA proportion tended to increase (Figure S4) and

549 periphyton SAFA proportions generally decreased. In contrast, benthic macroinvertebrate fatty  
550 acid class proportions tended to remain consistent across the entire gradient (Figure S4).

551  
552 For both periphyton and grazers, our analyses focused mainly on the fatty acids consistently  
553 associated with filamentous green algae (i.e., 18:3 $\omega$ 3, 18:1 $\omega$ 9, 18:2 $\omega$ 6, and 16:0) as well as  
554 diatoms (i.e., 20:5 $\omega$ 3, 16:1 $\omega$ 7, 14:0, and 16:0). For periphyton, the ratio of green  
555 filamentous:diatom-associated fatty acids significantly increased with an increasing PPCP  
556 concentration ( $R^2 = 0.62$ ;  $p = 0.04$ , Figure 7; S5) but not with an increasing IDW population ( $p =$   
557 0.08). Amphipod fatty acid ratios were not significantly related with either increasing IDW  
558 population or increasing PPCP concentrations (Figure 7; S6). When focusing solely on the  
559 essential fatty acids 18:3 $\omega$ 3, 18:2 $\omega$ 6, and 20:5 $\omega$ 3, the same pattern was observed in both  
560 periphyton ( $R^2 = 0.73$ ;  $p = 0.02$ ) and amphipods (Figure 7).

561  
562 **Discussion**  
563

564 Our combined results corroborate previous findings (e.g., Timoshkin et al., 2016; 2018) that  
565 sewage pollution is entering Lake Baikal's nearshore area and likely is responsible for changes in  
566 nearshore benthic communities. Unlike previous studies, we were able to incorporate highly  
567 specific indicators of sewage pollution and food web structure to offer direct, quantitative  
568 relationships between human development and ecological responses.

569  
570 *Relating human settlements to sewage indicator concentrations*  
571

572 In agreement with our expectations, some sewage pollution indicators in the nearshore of Lake  
573 Baikal were associated with size of and distance from human settlements. Total PPCP,  
574 macroinvertebrate  $\delta^{15}\text{N}$ , and, to some degree, total phosphorus concentrations increased with  
575 IDW population. These sewage gradients created by highly localized settlements are noteworthy  
576 considering that Baikal's shoreline, including our study area, is largely free of lakeside  
577 development (Moore et al. 2009). Furthermore, the use of sewage-associated indicators, such as  
578 PPCPs and  $\delta^{15}\text{N}$ , proved necessary for defining sewage gradients. The use of nutrients as  
579 indicators alone would not reveal sewage pollution gradients, since nutrients were not strongly  
580 correlated with IDW population and could come from diverse sources. For example, melting  
581 permafrost in Lake Baikal's watershed (Anisimov and Reneva 2006) and the Selenga River basin  
582 (Tornqvist et al. 2014) as well as climate-driven changes in mixing processes (Swann et al. 2020)  
583 have the potential to contribute substantial nutrient loadings to the nearshore. While nutrients  
584 also could be contributed by agriculture (Powers et al. 2016), atmospheric deposition (Galloway  
585 et al. 2004; Monteith et al. 2007; Stoddard et al. 2016), and changing terrestrial plant  
586 communities (Moran et al. 2012), these are not currently known to be major sources of elevated  
587 nutrients in the Baikal watershed, relative to sewage (Timoshkin et al., 2016, Timoshkin et al.,  
588 2018) and permafrost melt (Anisimov & Reneva, 2006).

589

590 This is the first known study to detect PPCPs in Lake Baikal, a voluminous lake in a largely  
591 unpopulated watershed. We detected PPCPs nearshore but not at our three offshore sites,  
592 suggesting that sewage inputs in Baikal become diluted as pollutants move out of the nearshore  
593 area. More generally, these results are important for lake monitoring, as PPCPs are robust  
594 indicators of sewage pollution. Beyond Lake Baikal, these data are important for understanding  
595 PPCPs' prevalence in lakes, as lakes have remained less represented in the PPCP literature in  
596 comparison to lotic and subsurface systems (Meyer et al. 2019). This literature imbalance creates  
597 opportunities to assess how PPCPs, and sewage pollution more broadly, may lead to differing  
598 ecological responses in lotic and lentic systems. As lakes tend to have longer hydraulic residence  
599 times relative to rivers and streams, pollutants may be more prone to accumulate (Yang et al.  
600 2018; Meyer et al. 2019). In the case of our data, comparing contemporaneous littoral and  
601 pelagic PPCP concentrations revealed littoral-pelagic sewage gradients, as PPCPs were  
602 degraded, metabolized or accumulated by biota, preserved within sediments, or diluted to  
603 undetectable concentrations. In the context of the entire lake, analyses of sediments have shown  
604 how PPCPs can remain within lake systems for decades, thereby enabling researchers to  
605 reconstruct histories of wastewater pollution in a system (Czekalski et al. 2015; Yang et al.  
606 2018).

607

608 Investigating PPCP concentrations across limnic environments could also establish how  
609 ecological communities respond differently not only to sewage but also to the PPCPs themselves.  
610 While we focus on PPCPs as indicators of sewage, previous studies have shown that PPCPs,  
611 even at concentrations we observed in Lake Baikal, can elicit biological responses from  
612 physiological (e.g., del Rey et al. 2011; Feijão et al. 2020) and behavioral (e.g., Brodin et al.  
613 2013; Dzieweczynski et al. 2016) levels to food webs (e.g., Lagesson et al. 2016; Richmond et  
614 al. 2018) and ecosystems (e.g., Rosi-Marshall et al. 2013; Richmond et al. 2019; Robson et al.  
615 2020). Although our study was not designed to evaluate the ecotoxicological effects of PPCPs  
616 themselves, future studies could potentially address effects of PPCPs on nearshore Baikal biota  
617 by using *in situ* sewage gradients as a guide.

618

619 In contrast to PPCP concentrations and  $\delta^{15}\text{N}$  values, microplastics were not associated with IDW  
620 population and may be poor proxies for sewage pollution in Lake Baikal. Additionally,  
621 microplastics may originate from non-sewage sources, such as agriculture (Steinmetz et al. 2016)  
622 and fish nets (Eerkes-Medrano et al. 2015). Because of their long degradation time (Brandon et  
623 al. 2016), microplastics can indicate accumulated pollution, which likely enables wider  
624 distribution from nearshore inputs to the offshore (Fischer et al. 2016; Hendrickson et al. 2018).  
625 Unlike microplastic concentrations identified in Lake Hovsgol (Free et al. 2014), Lake Superior  
626 (Hendrickson et al. 2018), or Lake Erie (Eriksen et al. 2013), microplastic concentrations in  
627 Baikal, as quantified by our methods, may be poor proxies for capturing pollution from  
628 seasonally varying human populations. It is worth noting that since the time of our field

629 sampling, evidence has accumulated that our methods likely dramatically underestimated  
630 microplastic abundance (Wang and Wang 2018; Brandon et al. 2020), and there is potential for  
631 the microplastics themselves to cause deleterious ecological responses. While we focus here on  
632 microplastics as an indicator of sewage pollution, microplastics are increasingly shown to disrupt  
633 food web dynamics by altering grazing patterns (Green 2016) and providing carbon substrate for  
634 microbial growth (Romera-Castillo et al. 2018). Although microplastics as measured on a  
635 volumetric basis in Lake Baikal are low relative other lakes worldwide, recent investigations of  
636 microplastics in Lake Baikal near Bolshie Koty (BK) used analogous methods and measured  
637 similar microplastic concentrations (Karnaukhov et al. 2020). When considering Lake Baikal's  
638 large volume, Karnaukhov et al. (2020) noted that the number of plastic pieces may well exceed  
639 those observed in other lakes, such as Lake Hovsgol. Together these growing uncertainties  
640 suggest that microplastic pollution in Baikal and elsewhere deserves increased attention.

641

#### 642 *Relating sewage indicators with benthic algal communities*

643

644 Congruent with our hypotheses, increasing sewage indicators tended to be associated with higher  
645 relative abundance of filamentous taxa in periphyton. Previous studies investigating Baikal's  
646 periphyton composition noted that areas adjacent to human development often had increased  
647 abundance of filamentous algae such as *Ulothrix* and *Spirogyra* (Timoshkin et al. 2016, 2018).  
648 Lake Baikal's southwestern shore historically experiences short *Ulothrix* blooms in late August  
649 (Kozhov 1963), potentially confounding sewage signals with an annually occurring  
650 phenomenon. Our data are consistent with the results of Timoshkin et al. (2016) and show that  
651 relative abundance of filamentous algae is greatest near areas of higher lakeside development.

652

653 While community composition shifted with increasing sewage indicator concentrations,  
654 periphyton  $\delta^{15}\text{N}$  values did not differ along our transect. Previous studies in marine (Gartner et  
655 al. 2002; Savage and Elmgren 2004; Risk et al. 2009) and freshwater (Wayland and Hobson  
656 2001; Camilleri and Ozersky 2019) systems have highlighted how sewage-associated  $\delta^{15}\text{N}$  can  
657 increase in algal samples and even throughout the food web. Like PPCPs in our study,  $\delta^{15}\text{N}$   
658 values are often most enriched near the source of sewage pollution and can decrease over several  
659 kilometers (Savage and Elmgren 2004), with concentrations varying based on species-specific  
660 uptake rates and advective, dispersive, and diffusive transport (Gartner et al. 2002). While  
661 previous studies using  $\delta^{15}\text{N}$  signatures in macroalgae and vascular macrophytes have  
662 successfully tracked sewage gradients (Cole et al. 2004), periphyton  $\delta^{15}\text{N}$  as a sewage indicator  
663 potentially can be confounded by terrestrial  $\delta^{15}\text{N}$  contributions such as through agricultural  
664 runoff (Chang et al. 2012). In our study, periphyton  $\delta^{15}\text{N}$  signatures may be explained by  
665 periphyton's typically high cell turnover rates (e.g., days; Swamikannu and Hoagland 1989)  
666 dampening isotopic patterns,  $\delta^{15}\text{N}$ -accumulating algal taxa being grazed more readily by  
667 macroinvertebrates (Rosenberger et al. 2008), or co-limitation dynamics between ammonium and  
668 nitrate (York et al. 2007; Piñón-Gimate et al. 2009).

669  
670 Fatty acid analyses suggested that changes in periphyton community composition altered the  
671 nutritional quality of periphyton across the pollution gradient. Periphyton fatty acid profiles from  
672 sites with higher sewage pollution had higher levels of 18:3 $\omega$ 3, 18:1 $\omega$ 9, 18:2 $\omega$ 6, and 16:0  
673 relative to 20:5 $\omega$ 3, 16:1 $\omega$ 7, 16:0, and 14:0 fatty acids. This pattern likely reflects the higher  
674 abundance of green algae relative to diatoms (Iverson et al. 2004; Osipova et al. 2009; Taipale et  
675 al. 2013; Galloway and Winder 2015; Shishlyannikov et al. 2018), which we observed from our  
676 periphyton community composition analysis (Figure 3). Together, our periphyton composition  
677 and fatty acid results suggest that Baikal's nearshore periphyton communities near human  
678 lakeside developments are more dominated by filamentous green algae, and therefore, have  
679 lower nutritional content.  
680  
681 Among the array of fatty acids synthesized in algal communities, essential fatty acids (EFAs) are  
682 most likely to be taxonomically associated with, and influenced by, changing community  
683 composition. EFAs are a subgroup of polyunsaturated fatty acids (PUFAs) that are prone to  
684 accumulating in organisms (see Kelly & Scheibling, 2012). Among the eight common EFAs  
685 (Taipale et al. 2013), 18:3 $\omega$ 3, 18:2 $\omega$ 6, and 20:5 $\omega$ 3 had the highest coefficient of variation  
686 between sites. Because these three EFAs demonstrated the greatest variation between sites, our  
687 analyses focused on how their relative abundances related to PPCP concentrations and IDW  
688 populations. The fatty acids 18:3 $\omega$ 3 and 18:2 $\omega$ 6 have been previously associated with  
689 filamentous algae, such as Baikalian *Ulothrix* (Osipova et al. 2009), whereas 20:5 $\omega$ 3 have  
690 previously been associated with Baikalian diatoms (Shishlyannikov et al. 2018). Comparing the  
691 ratio of filamentous green algae to diatoms could therefore function as proxy for each algal  
692 taxon's relative abundance and potentially offer insights into feeding patterns for the grazers.  
693  
694 *Relating sewage indicators with macroinvertebrate feeding guilds*  
695  
696 In assessing benthic consumer communities' responses to changing periphyton, our data suggest  
697 macroinvertebrate guilds reshape with increasing sewage pollution. Our results support the  
698 general conclusion of Timoshkin et al. (2016) that Baikalian mollusk abundance tends to  
699 decrease with increasing sewage pollution. Decreased mollusk abundance may have several  
700 causes, including low tolerance for increased concentrations of PPCPs or other components of  
701 sewage (e.g., Hollingsworth et al. 2002, Timoshkin et al. 2016), inability to consume filamentous  
702 algae (Mazzella and Russo 1989), or filamentous algae not offering the proper nutrition (Lowe  
703 and Hunter 1988). In contrast to mollusks, amphipods were generally prevalent at all littoral sites  
704 regardless of sewage indicator concentrations. *Brandtia* spp. was the only amphipod genus less  
705 abundant with sewage indicator signals. This genus tends to be associated with endemic sponges  
706 (Taakhteev & Didorenko, 2015), which may also be decreasing in abundance near areas of  
707 lakeside development (Timoshkin et al., 2016). *Eulimnogammarus* spp., one of the most speciose  
708 Baikal genera (Takhteev and Didorenko 2015), was prevalent at all sites, and  $\delta^{15}\text{N}$  values in its

tissue increased slightly but significantly with increasing IDW population. Unlike periphyton, amphipods' increasing  $\delta^{15}\text{N}$  values may relate to amphipods having longer cellular turnover rates (e.g., weeks; McIntyre and Flecker 2006) relative to periphyton. Consequently, amphipods' enhanced  $\delta^{15}\text{N}$  values suggest that sewage-derived nutrients are being incorporated into the food web. While we did not test amphipod tissues for other sewage indicators such as PPCPs and microplastics, the potential for PPCPs to bioaccumulate and biomagnify in food webs has been recently demonstrated, with ecological ramifications remaining uncertain (Lagesson et al., 2016; Richmond et al., 2018). These combined results suggest that mollusk abundance and amphipod  $\delta^{15}\text{N}$  values may be longer-term indicators of sewage pollution in Baikal.

In contrast to variation in  $\delta^{15}\text{N}$  values, amphipod fatty acid profiles did not differ markedly between sites (Figure 7). Amphipods from all collected sites expressed consistent 20:5 $\omega$ 3 signatures relative to 18:3 $\omega$ 3 and 18:2 $\omega$ 6. Consumers usually accumulate fatty acids from their food source. Yoshii's (1999) study as well as our own stable isotope data suggest that Baikal's benthic, littoral amphipods are likely a combination of grazers and omnivores. Because fatty acid profiles in amphipods largely reflected fatty acid signatures in periphyton, our data suggest that amphipods likely continue grazing on periphyton, despite the food resource changing in community composition and nutritional content. As a consequence, amphipods may be compensating for the shifting nutritional quality of periphyton through at least two potential mechanisms. First, amphipods may selectively consume diatoms as opposed to filamentous algae, meaning diatom relative abundance could decrease both from increased grazing and lesser efficiency at taking up nutrients relative to filamentous taxa. Second, amphipods themselves (e.g., Desvillettes et al. 1997; Castell et al. 2004) or heterotrophic symbionts (Klein Breteler et al. 1999; Veloza et al. 2006; Hiltunen et al. 2017) may upgrade fatty acids by investing energy to convert C18 fatty acids to C20 fatty acids. Regardless of the exact mechanism, our data suggest that food web interactions would change with increasing sewage pollution and may imply a net energetic cost through amphipods' differential grazing patterns.

*Conclusions*

Over the past decade, Lake Baikal has shown signs of nearshore eutrophication, despite the pelagic zone remaining ultra-oligotrophic. While Baikal receives nutrients from multiple sources, sewage-specific indicators used in this study implicate wastewater pollution as one of the sources. Our results corroborate work by Timoshkin et al. (2016, 2018), demonstrating how patchy hot spots of lakeside development at Baikal can create gradients in sewage concentrations and ecological responses. Unlike previous studies, our approach pairs community abundance data (i.e., periphyton and macroinvertebrate counts) and nuanced dietary tracers (i.e., fatty acids) to assess benthic community and food web consequences of sewage pollution. While sewage pollution may lead to changing resources for macroinvertebrate grazers, Baikal's amphipods appear to be compensating either (1) by selectively grazing on diatoms or (2) by consuming less

749 desirable food and upgrading fatty acids. In both cases, our results suggest shifting community  
750 interactions and may imply a net energetic cost for amphipods, as they expend energy either by  
751 foraging selectively for diatoms or by catabolizing certain essential fatty acids.

752

753 *Future trajectories: a call for increased nearshore monitoring*

754

755 Our results underscore the importance of nearshore monitoring in detecting sewage pollution in  
756 large lakes. Lake Baikal is considered ultra-oligotrophic based on pelagic sampling (Yoshida et  
757 al. 2003; O'Donnell et al. 2017), but nearshore hot spots of eutrophication are developing  
758 throughout the lake (Timoshkin et al. 2016, 2018). While pelagic samples are representative of  
759 the lake's overall status, nearshore sampling aids managers in identifying pollution loading  
760 before the entire system is affected (Jacoby et al. 1991; Lambert et al. 2008; Hampton et al.  
761 2011). Beyond Baikal, several large, deep, oligotrophic lakes have likewise experienced  
762 localized sewage pollution with nearshore biological responses, despite pelagic measurements  
763 suggesting oligotrophic status (e.g., Jacoby et al. 1991, Rosenberger et al. 2008; Hampton et al.,  
764 2011). Once eutrophication of the open water has occurred, mitigation can involve complex  
765 socio-economic factors (Carpenter et al. 1999), require system-specific information (Jeppesen et  
766 al. 2005), and necessitate long-term strategies (Tong et al. 2020). Because nutrients may enter  
767 systems from numerous sources, incorporating sewage specific indicators, such as PPCPs, may  
768 be necessary. PPCP sampling has the potential to not only identify sewage-associated nutrient  
769 pollution but also assess heterogeneities in sewage loading along a shoreline. When PPCP data  
770 are paired with co-located benthic community composition and food web data, managers can  
771 take system-specific actions to mitigate ecological consequences before sewage concentrations  
772 are detected throughout the lake. Across larger spatial and temporal scales, these paired PPCP-  
773 biological samples have potential to offer a synoptic view of the impacts of sewage pollution,  
774 enabling regional and local monitoring to coordinate mitigation strategies

775

776

## Works Cited

7

779 Anderson, M. J. 2001. A new method for non-parametric multivariate analysis of variance.

780 Austral Ecology 26: 32–46. doi:10.1111/j.1442-9993.2001.01070.pp.x

781 Andersson, E., and A.-K. Brunberg. 2006. Inorganic nutrient acquisition in a shallow clearwater  
782 lake – dominance of benthic microbiota. *Aquatic Sciences* **68**: 172–180.  
783 doi:10.1007/s00027-006-0805-x

784 Anisimov, O., and S. Reneva. 2006. Permafrost and Changing Climate: The Russian  
785 Perspective. *Ambio* **35**: 169–175.

786 Barnes, D. K. A., F. Galgani, R. C. Thompson, and M. Barlaz. 2009. Accumulation and  
787 fragmentation of plastic debris in global environments. *Philos Trans R Soc Lond B Biol  
788 Sci* **364**: 1985–1998. doi:10.1098/rstb.2008.0205

789 Bendz, D., N. A. Paxéus, T. R. Ginn, and F. J. Loge. 2005. Occurrence and fate of  
790 pharmaceutically active compounds in the environment, a case study: Höje River in  
791 Sweden. *Journal of Hazardous Materials* **122**: 195–204.  
792 doi:10.1016/j.jhazmat.2005.03.012

793 Brandon, J. A., A. Freibott, and L. M. Sala. 2020. Patterns of suspended and salp-ingested  
794 microplastic debris in the North Pacific investigated with epifluorescence microscopy.

795 Limnology and Oceanography Letters 5: 46–53. doi:10.1002/lol2.10127

796 Brandon, J., M. Goldstein, and M. D. Ohman. 2016. Long-term aging and degradation of  
797 microplastic particles: Comparing *in situ* oceanic and experimental weathering patterns.  
798 *Marine Pollution Bulletin* **110**: 299–308. doi:10.1016/j.marpolbul.2016.06.048

799 Brodin, T., J. Fick, M. Jonsson, and J. Klaminder. 2013. Dilute Concentrations of a Psychiatric  
800 Drug Alter Behavior of Fish from Natural Populations. *Science* **339**: 814–815.  
801 doi:10.1126/science.1226850

- 802 Camilleri, A. C., and T. Ozersky. 2019. Large variation in periphyton  $\delta^{13}\text{C}$  and  $\delta^{15}\text{N}$  values in  
803 the upper Great Lakes: Correlates and implications. *Journal of Great Lakes Research*  
804 **45**: 986–990. doi:10.1016/j.jglr.2019.06.003
- 805 Carpenter, S. R., D. Ludwig, and W. A. Brock. 1999. Management of Eutrophication for Lakes  
806 Subject to Potentially Irreversible Change. *Ecological Applications* **9**: 751–771.  
807 doi:10.2307/2641327
- 808 Castell, J. D., E. J. Kennedy, S. M. C. Robinson, G. J. Parsons, T. J. Blair, and E. Gonzalez-  
809 Duran. 2004. Effect of dietary lipids on fatty acid composition and metabolism in juvenile  
810 green sea urchins (*Strongylocentrotus droebachiensis*). *Aquaculture* **242**: 417–435.  
811 doi:10.1016/j.aquaculture.2003.11.003
- 812 Chang, H.-Y., S.-H. Wu, K.-T. Shao, and others. 2012. Longitudinal variation in food sources  
813 and their use by aquatic fauna along a subtropical river in Taiwan. *Freshwater Biology*  
814 **57**: 1839–1853. doi:10.1111/j.1365-2427.2012.02843.x
- 815 Clarke, K. R. 1993. Non-parametric multivariate analyses of changes in community structure.  
816 *Australian Journal of Ecology* **18**: 117–143. doi:<https://doi.org/10.1111/j.1442-9993.1993.tb00438.x>
- 817 Cole, M. L., I. Valiela, K. D. Kroeger, and others. 2004. Assessment of a  $\delta^{15}\text{N}$  isotopic  
818 method to indicate anthropogenic eutrophication in aquatic ecosystems. *J. Environ.  
819 Qual.* **33**: 124–132. doi:10.2134/jeq2004.1240
- 820 Costanzo, S. D., M. J. O'Donohue, W. C. Dennison, N. R. Loneragan, and M. Thomas. 2001. A  
821 New Approach for Detecting and Mapping Sewage Impacts. *Marine Pollution Bulletin* **42**:  
822 149–156. doi:10.1016/S0025-326X(00)00125-9
- 823 Craine, J. M., A. J. Elmore, L. Wang, and others. 2018. Isotopic evidence for oligotrophication of  
824 terrestrial ecosystems. *Nature Ecology & Evolution* **2**: 1735–1744. doi:10.1038/s41559-  
825 018-0694-0

- 827 Czekalski, N., R. Sigdel, J. Birtel, B. Matthews, and H. Bürgmann. 2015. Does human activity  
828 impact the natural antibiotic resistance background? Abundance of antibiotic resistance  
829 genes in 21 Swiss lakes. *Environment International* **81**: 45–55.  
830 doi:10.1016/j.envint.2015.04.005
- 831 D'Alessio, M., S. Onanong, D. D. Snow, and C. Ray. 2018. Occurrence and removal of  
832 pharmaceutical compounds and steroids at four wastewater treatment plants in Hawai'i  
833 and their environmental fate. *Science of The Total Environment* **631–632**: 1360–1370.  
834 doi:10.1016/j.scitotenv.2018.03.100
- 835 Dalsgaard, J., M. St. John, G. Kattner, D. Müller-Navarra, and W. Hagen. 2003. Fatty acid  
836 trophic markers in the pelagic marine environment, p. 225–340. *In* Advances in Marine  
837 Biology. Elsevier.
- 838 Desvilettes, Ch., G. Bourdier, and J. Ch. Breton. 1997. On the occurrence of a possible  
839 bioconversion of linolenic acid into docosahexaenoic acid by the copepod *Eucyclops*  
840 *serrulatus* fed on microalgae. *J Plankton Res* **19**: 273–278. doi:10.1093/plankt/19.2.273
- 841 Dziewczynski, T. L., B. A. Campbell, and J. L. Kane. 2016. Dose-dependent fluoxetine effects  
842 on boldness in male Siamese fighting fish. *Journal of Experimental Biology* **219**: 797–  
843 804. doi:10.1242/jeb.132761
- 844 Eerkes-Medrano, D., R. C. Thompson, and D. C. Aldridge. 2015. Microplastics in freshwater  
845 systems: A review of the emerging threats, identification of knowledge gaps and  
846 prioritisation of research needs. *Water Research* **75**: 63–82.  
847 doi:10.1016/j.watres.2015.02.012
- 848 Eriksen, M., S. Mason, S. Wilson, C. Box, A. Zellers, W. Edwards, H. Farley, and S. Amato.  
849 2013. Microplastic pollution in the surface waters of the Laurentian Great Lakes. *Marine  
850 Pollution Bulletin* **77**: 177–182. doi:10.1016/j.marpolbul.2013.10.007

- 851 Feijão, E., R. Cruz de Carvalho, I. A. Duarte, and others. 2020. Fluoxetine Arrests Growth of the  
852 Model Diatom *Phaeodactylum tricornutum* by Increasing Oxidative Stress and Altering  
853 Energetic and Lipid Metabolism. *Front Microbiol* **11**. doi:10.3389/fmicb.2020.01803
- 854 Fellows, I., and using the Jm. library by J. P. Stotz. 2019. OpenStreetMap: Access to Open  
855 Street Map Raster Images.,
- 856 Firke, S. 2020. janitor: Simple Tools for Examining and Cleaning Dirty Data.,
- 857 Fischer, E. K., L. Paglialonga, E. Czech, and M. Tamminga. 2016. Microplastic pollution in lakes  
858 and lake shoreline sediments – A case study on Lake Bolsena and Lake Chiusi (central  
859 Italy). *Environmental Pollution* **213**: 648–657. doi:10.1016/j.envpol.2016.03.012
- 860 Focazio, M. J., D. W. Kolpin, K. K. Barnes, E. T. Furlong, M. T. Meyer, S. D. Zaugg, L. B.  
861 Barber, and M. E. Thurman. 2008. A national reconnaissance for pharmaceuticals and  
862 other organic wastewater contaminants in the United States - II) Untreated drinking  
863 water sources. *SCIENCE OF THE TOTAL ENVIRONMENT* **402**: 201–216.  
864 doi:10.1016/j.scitotenv.2008.02.021
- 865 Free, C. M., O. P. Jensen, S. A. Mason, M. Eriksen, N. J. Williamson, and B. Boldgiv. 2014.  
866 High-levels of microplastic pollution in a large, remote, mountain lake. *Marine Pollution  
867 Bulletin* **85**: 156–163. doi:10.1016/j.marpolbul.2014.06.001
- 868 Galloway, A. W. E., and M. Winder. 2015. Partitioning the Relative Importance of Phylogeny  
869 and Environmental Conditions on Phytoplankton Fatty Acids. *PLOS ONE* **10**: e0130053.  
870 doi:10.1371/journal.pone.0130053
- 871 Galloway, J. N., F. J. Dentener, D. G. Capone, and others. 2004. Nitrogen Cycles: Past,  
872 Present, and Future. *Biogeochemistry* **70**: 153–226. doi:10.1007/s10533-004-0370-0
- 873 Garnier, S. 2018. viridis: Default Color Maps from “matplotlib.”
- 874 Gartner, A., P. Lavery, and A. J. Smit. 2002. Use of delta N-15 signatures of different functional  
875 forms of macroalgae and filter-feeders to reveal temporal and spatial patterns in sewage  
876 dispersal. *Mar. Ecol.-Prog. Ser.* **235**: 63–73. doi:10.3354/meps235063

- 877 Green, D. S. 2016. Effects of microplastics on European flat oysters, *Ostrea edulis* and their  
878 associated benthic communities. *Environmental Pollution* **216**: 95–103.  
879 doi:10.1016/j.envpol.2016.05.043
- 880 Guzzo, M. M., G. D. Haffner, S. Sorge, S. A. Rush, and A. T. Fisk. 2011. Spatial and temporal  
881 variabilities of  $\delta^{13}\text{C}$  and  $\delta^{15}\text{N}$  within lower trophic levels of a large lake: implications for  
882 estimating trophic relationships of consumers. *Hydrobiologia* **675**: 41–53.  
883 doi:10.1007/s10750-011-0794-1
- 884 Hadwen, W. L., and S. E. Bunn. 2005. Food web responses to low-level nutrient and  $\text{N}^+$ -  
885 tracer additions in the littoral zone of an oligotrophic dune lake. *Limnology and*  
886 *Oceanography* **50**: 1096.
- 887 Hampton, S. E., S. C. Fradkin, P. R. Leavitt, and E. E. Rosenberger. 2011. Disproportionate  
888 importance of nearshore habitat for the food web of a deep oligotrophic lake. *Marine and*  
889 *Freshwater Research* **62**: 350. doi:10.1071/MF10229
- 890 Hampton, S. E., S. McGowan, T. Ozersky, and others. 2018. Recent ecological change in  
891 ancient lakes. *Limnology and Oceanography* **63**: 2277–2304. doi:10.1002/lo.10938
- 892 Hanvey, J. S., P. J. Lewis, J. L. Lavers, N. D. Crosbie, K. Pozo, and B. O. Clarke. 2017. A  
893 review of analytical techniques for quantifying microplastics in sediments. *Anal. Methods*  
894 **9**: 1369–1383. doi:10.1039/C6AY02707E
- 895 Hendrickson, E., E. C. Minor, and K. Schreiner. 2018. Microplastic Abundance and Composition  
896 in Western Lake Superior As Determined via Microscopy, Pyr-GC/MS, and FTIR.  
897 *Environ. Sci. Technol.* **52**: 1787–1796. doi:10.1021/acs.est.7b05829
- 898 Hester, J., and H. Wickham. 2019. fs: Cross-Platform File System Operations Based on “libuv,.”
- 899 Hiltunen, M., M. Honkanen, S. Taipale, U. Strandberg, and P. Kankaala. 2017. Trophic  
900 upgrading via the microbial food web may link terrestrial dissolved organic matter to  
901 *Daphnia*. *J Plankton Res* **39**: 861–869. doi:10.1093/plankt/fbx050

- 902 Hollingsworth, R. G., J. W. Armstrong, and E. Campbell. 2002. Caffeine as a repellent for slugs  
903 and snails. *Nature* **417**: 915–916. doi:10.1038/417915a
- 904 Interfax-Tourism. 2018. Байкал с января по август 2018 года посетили 1,2 миллиона  
905 туристов (1.2 million tourists vistied Baikal from January through August 2018). Interfax-  
906 Tourism, October 25
- 907 Iverson, S. J., C. Field, W. D. Bowen, and W. Blanchard. 2004. Quantitative Fatty Acid  
908 Signature Analysis: A New Method of Estimating Predator Diets. *Ecological Monographs*  
909 **74**: 211–235. doi:10.1890/02-4105
- 910 Izhboldina, L. A. 2007. Guide and Key to Benthic and Periphyton Algae of Lake Baikal (meio-  
911 and macrophytes) with Brief Notes on Their Ecology, Nauka-Centre.
- 912 Jacoby, J. M., D. D. Bouchard, and C. R. Patmont. 1991. Response of Periphyton to Nutrient  
913 Enrichment in Lake Chelan, WA. *Lake and Reservoir Management* **7**: 33–43.  
914 doi:10.1080/07438149109354252
- 915 Jeppesen, E., M. Søndergaard, J. P. Jensen, and others. 2005. Lake responses to reduced  
916 nutrient loading – an analysis of contemporary long-term data from 35 case studies.  
917 *Freshwater Biology* **50**: 1747–1771. doi:10.1111/j.1365-2427.2005.01415.x
- 918 Johnson, R. A., and D. V. Wichern. 2007. *Applied Multivariate Statistical Analysis*, 6th ed.  
919 Prentice Hall.
- 920 Karnaughov, D., S. Biritskaya, E. Dolinskaya, M. Teplykh, N. Silenko, Y. Ermolaeva, and E.  
921 Silow. 2020. POLLUTION BY MACRO- AND MICROPLASTIC OF LARGE  
922 LACUSTRINE ECOSYSTEMS IN EASTERN ASIA. *Pollution Research* **2**: 353–355.
- 923 Karnjanapiboonwong, A., A. N. Morse, J. D. Maul, and T. A. Anderson. 2010. Sorption of  
924 estrogens, triclosan, and caffeine in a sandy loam and a silt loam soil. *Journal of Soils  
925 and Sediments* **10**: 1300–1307. doi:10.1007/s11368-010-0223-5
- 926 Kassambara, A. 2019. *ggpubr: “ggplot2” Based Publication Ready Plots.*,

- 927 Kassambara, A., and F. Mundt. 2019. factoextra: Extract and Visualize the Results of  
928 Multivariate Data Analyses.,
- 929 Kaufman, L., and P. J. Rousseeuw. 2005. Finding Groups in Data: An Introduction to Cluster  
930 Analysis, 1st Edition. Wiley-Interscience.
- 931 Kelly, J. R., and R. E. Scheibling. 2012. Fatty acids as dietary tracers in benthic food webs.  
932 Marine Ecology Progress Series **446**: 1–22. doi:10.3354/meps09559
- 933 Klein Breteler, W. C. M., N. Schogt, M. Baas, S. Schouten, and G. W. Kraay. 1999. Trophic  
934 upgrading of food quality by protozoans enhancing copepod growth: role of essential  
935 lipids. Marine Biology **135**: 191–198. doi:10.1007/s002270050616
- 936 Klein, S., E. Worch, and T. P. Knepper. 2015. Occurrence and Spatial Distribution of  
937 Microplastics in River Shore Sediments of the Rhine-Main Area in Germany. Environ.  
938 Sci. Technol. **49**: 6070–6076. doi:10.1021/acs.est.5b00492
- 939 Kolpin, D. W., E. T. Furlong, M. T. Meyer, E. M. Thurman, S. D. Zaugg, L. B. Barber, and H. T.  
940 Buxton. 2002. Pharmaceuticals, Hormones, and Other Organic Wastewater  
941 Contaminants in U.S. Streams, 1999–2000: A National Reconnaissance. Environmental  
942 Science & Technology **36**: 1202–1211. doi:10.1021/es011055j
- 943 Kozhov, M. M. 1963. Lake Baikal and its Life, Springer Science & Business Media.
- 944 Kozhova, O. M., and L. R. Izmest'eva. 1998. Lake Baikal: Evolution and Biodiversity, Backhuys  
945 Publishers.
- 946 Kravtsova, L. S., L. A. Izhboldina, I. V. Khanaev, and others. 2014. Nearshore benthic blooms of  
947 filamentous green algae in Lake Baikal. Journal of Great Lakes Research **40**: 441–448.  
948 doi:10.1016/j.jglr.2014.02.019
- 949 Lagesson, A., J. Fahlman, T. Brodin, J. Fick, M. Jonsson, P. Byström, and J. Klaminder. 2016.  
950 Bioaccumulation of five pharmaceuticals at multiple trophic levels in an aquatic food web  
951 - Insights from a field experiment. Science of The Total Environment **568**: 208–215.  
952 doi:10.1016/j.scitotenv.2016.05.206

- 953     Lambert, D., A. Cattaneo, and R. Carignan. 2008. Periphyton as an early indicator of  
954                 perturbation in recreational lakes. *Can. J. Fish. Aquat. Sci.* **65**: 258–265.  
955                 doi:10.1139/f07-168
- 956     Legendre, P., and L. Legendre. 2012. *Numerical Ecology*, 3rd ed. Elsevier.
- 957     Li, J., C. Green, A. Reynolds, H. Shi, and J. M. Rotchell. 2018. Microplastics in mussels  
958                 sampled from coastal waters and supermarkets in the United Kingdom. *Environmental  
959                 Pollution* **241**: 35–44. doi:10.1016/j.envpol.2018.05.038
- 960     Lorenzen, C. J. 1967. Determination of Chlorophyll and Pheo-Pigments: Spectrophotometric  
961                 Equations1. *Limnology and Oceanography* **12**: 343–346.  
962                 doi:<https://doi.org/10.4319/lo.1967.12.2.0343>
- 963     Lowe, R. L., and R. D. Hunter. 1988. Effect of Grazing by *Physa integra* on Periphyton  
964                 Community Structure. *Journal of the North American Benthological Society* **7**: 29–36.  
965                 doi:10.2307/1467828
- 966     Maechler, M., P. Rousseeuw, A. Struyf, M. Hubert, and K. Hornik. 2019. *cluster: Cluster  
967                 Analysis Basics and Extensions*,.
- 968     Mazzella, L., and G. F. Russo. 1989. Grazing effect of two *Gibbula* species (Mollusca,  
969                 Archaeogastropoda) on the epiphytic community of *Posidonia oceanica* leaves.
- 970     McIntyre, P. B., and A. S. Flecker. 2006. Rapid turnover of tissue nitrogen of primary consumers  
971                 in tropical freshwaters. *Oecologia* **148**: 12–21. doi:10.1007/s00442-005-0354-3
- 972     Meyer, M. F., T. Ozersky, K. H. Woo, and others. 2020. A unified dataset of co-located sewage  
973                 pollution, periphyton, and benthic macroinvertebrate community and food web structure  
974                 from Lake Baikal  
975                 (Siberia).doi:10.6073/PASTA/76F43144015EC795679BAC508EFA044B
- 976     Meyer, M. F., S. M. Powers, and S. E. Hampton. 2019. An Evidence Synthesis of  
977                 Pharmaceuticals and Personal Care Products (PPCPs) in the Environment: Imbalances

978 among Compounds, Sewage Treatment Techniques, and Ecosystem Types. Environ.  
979 Sci. Technol. **53**: 12961–12973. doi:10.1021/acs.est.9b02966

980 Meyer, M., T. Ozersky, K. Woo, A. W. E. Galloway, M. R. Brousil, and S. Hampton. 2015. Baikal  
981 Food Webs.doi:10.17605/OSF.IO/9TA8Z

982 Monteith, D. T., J. L. Stoddard, C. D. Evans, and others. 2007. Dissolved organic carbon trends  
983 resulting from changes in atmospheric deposition chemistry. Nature **450**: 537–540.  
984 doi:10.1038/nature06316

985 Moore, J. W., D. E. Schindler, M. D. Scheuerell, D. Smith, and J. Frogge. 2003. Lake  
986 eutrophication at the urban fringe, Seattle region, USA. AMBIO: A Journal of the Human  
987 Environment **32**: 13–18.

988 Moore, M. V., S. E. Hampton, L. R. Izmest'eva, E. A. Silow, E. V. Peshkova, and B. K. Pavlov.  
989 2009. Climate Change and the World's "Sacred Sea"-Lake Baikal, Siberia. Bioscience  
990 **59**: 405–417. doi:10.1525/bio.2009.59.5.8

991 Moran, P. W., S. E. Cox, S. S. Embrey, R. L. Huffman, T. D. Olsen, and S. C. Fradkin. 2012.  
992 Sources and Sinks of Nitrogen and Phosphorus in a Deep, Oligotrophic Lake, Lake  
993 Crescent, Olympic National Park, Washington. US Geological Survey.

994 O'Donnell, D. R., P. Wilburn, E. A. Silow, L. Y. Yampolsky, and E. Litchman. 2017. Nitrogen and  
995 phosphorus colimitation of phytoplankton in Lake Baikal: Insights from a spatial survey  
996 and nutrient enrichment experiments. Limnology and Oceanography **62**: 1383–1392.  
997 doi:10.1002/leo.10505

998 Oksanen, J., F. G. Blanchet, M. Friendly, and others. 2019. vegan: Community Ecology  
999 Package,.

1000 Osipova, S., L. Dudareva, N. Bondarenko, A. Nasarova, N. Sokolova, L. Obolkina, O. Glyzina,  
1001 and O. Timoshkin. 2009. Temporal variation in fatty acid composition of *Ulothrix zonata*  
1002 (Chlorophyta) from ice and benthic communities of Lake Baikal. Phycologia **48**: 130–  
1003 135.

- 1004 Ozersky, T., E. A. Volkova, N. A. Bondarenko, O. A. Timoshkin, V. V. Malnik, V. M. Domysheva,  
1005 and S. E. Hampton. 2018. Nutrient limitation of benthic algae in Lake Baikal, Russia.  
1006 Freshwater Science **37**: 472–482. doi:10.1086/699408
- 1007 Parsons, T. R., and J. D. H. Strickland. 1963. Discussion of spectrophotometric determination of  
1008 marine-plant pigments, with revised equations for ascertaining chlorophylls and  
1009 carotenoids. Journal of Marine Research.
- 1010 Pebesma, E. 2018. Simple Features for R: Standardized Support for Spatial Vector Data. The R  
1011 Journal **10**: 439–446. doi:10.32614/RJ-2018-009
- 1012 Piñón-Gimate, A., M. F. Soto-Jiménez, M. J. Ochoa-Izaguirre, E. García-Pagés, and F. Páez-  
1013 Osuna. 2009. Macroalgae blooms and δ15N in subtropical coastal lagoons from the  
1014 Southeastern Gulf of California: Discrimination among agricultural, shrimp farm and  
1015 sewage effluents. Marine Pollution Bulletin **58**: 1144–1151.  
1016 doi:10.1016/j.marpolbul.2009.04.004
- 1017 Powers, S. M., T. W. Bruylants, T. P. Burt, and others. 2016. Long-term accumulation and  
1018 transport of anthropogenic phosphorus in three river basins. Nature Geoscience **9**: 353–  
1019 356. doi:10.1038/ngeo2693
- 1020 R Core Team. 2019. R: A Language and Environment for Statistical Computing.,  
1021 del Rey, Z. R., E. F. Granek, and B. A. Buckley. 2011. Expression of HSP70 in *Mytilus*  
1022 *californianus* following exposure to caffeine. Ecotoxicology **20**: 855–861.  
1023 doi:10.1007/s10646-011-0649-6
- 1024 Richmond, E. K., E. J. Rosi, A. J. Reisinger, B. R. Hanrahan, R. M. Thompson, and M. R.  
1025 Grace. 2019. Influences of the antidepressant fluoxetine on stream ecosystem function  
1026 and aquatic insect emergence at environmentally realistic concentrations. Journal of  
1027 Freshwater Ecology **34**: 513–531. doi:10.1080/02705060.2019.1629546

- 1028 Richmond, E. K., E. J. Rosi, D. M. Walters, J. Fick, S. K. Hamilton, T. Brodin, A. Sundelin, and  
1029 M. R. Grace. 2018. A diverse suite of pharmaceuticals contaminates stream and riparian  
1030 food webs. *Nature Communications* **9**: 4491. doi:10.1038/s41467-018-06822-w
- 1031 Risk, M. J., B. E. Lapointe, O. A. Sherwood, and B. J. Bedford. 2009. The use of  $\delta^{15}\text{N}$  in  
1032 assessing sewage stress on coral reefs. *Marine Pollution Bulletin* **58**: 793–802.  
1033 doi:10.1016/j.marpolbul.2009.02.008
- 1034 Robson, S. V., E. J. Rosi, E. K. Richmond, and M. R. Grace. 2020. Environmental  
1035 concentrations of pharmaceuticals alter metabolism, denitrification, and diatom  
1036 assemblages in artificial streams. *Freshwater Science* **39**: 256–267. doi:10.1086/708893
- 1037 Romera-Castillo, C., M. Pinto, T. M. Langer, X. A. Álvarez-Salgado, and G. J. Herndl. 2018.  
1038 Dissolved organic carbon leaching from plastics stimulates microbial activity in the  
1039 ocean. *Nat Commun* **9**: 1–7. doi:10.1038/s41467-018-03798-5
- 1040 Rosenberger, E. E., S. E. Hampton, S. C. Fradkin, and B. P. Kennedy. 2008. Effects of  
1041 shoreline development on the nearshore environment in large deep oligotrophic lakes.  
1042 *Freshwater Biology* **53**: 1673–1691. doi:10.1111/j.1365-2427.2008.01990.x
- 1043 Rosi-Marshall, E. J., D. W. Kincaid, H. A. Bechtold, T. V. Royer, M. Rojas, and J. J. Kelly. 2013.  
1044 Pharmaceuticals suppress algal growth and microbial respiration and alter bacterial  
1045 communities in stream biofilms. *Ecological Applications* **23**: 583–593. doi:10.1890/12-  
1046 0491.1
- 1047 Rosi-Marshall, E. J., and T. V. Royer. 2012. Pharmaceutical Compounds and Ecosystem  
1048 Function: An Emerging Research Challenge for Aquatic Ecologists. *Ecosystems* **15**:  
1049 867–880. doi:10.1007/s10021-012-9553-z
- 1050 Sargent, J. R., and S. Falk-Petersen. 1988. The lipid biochemistry of calanoid copepods.  
1051 *Hydrobiologia* **167–168**: 101–114. doi:10.1007/BF00026297

- 1052 Savage, C., and R. Elmgren. 2004. MACROALGAL (*FUCUS VESICULOSUS*)  $\delta^{15}\text{N}$  VALUES  
1053 TRACE DECREASE IN SEWAGE INFLUENCE. *Ecological Applications* **14**: 517–526.  
1054 doi:10.1890/02-5396
- 1055 Schram, J. B., J. N. Kobelt, M. N. Dethier, and A. W. E. Galloway. 2018. Trophic Transfer of  
1056 Macroalgal Fatty Acids in Two Urchin Species: Digestion, Egestion, and Tissue Building.  
1057 *Front. Ecol. Evol.* **6**. doi:10.3389/fevo.2018.00083
- 1058 Shishlyannikov, S. M., A. A. Nikonova, Y. S. Bukin, and A. G. Gorshkov. 2018. Fatty acid trophic  
1059 markers in Lake Baikal phytoplankton: A comparison of endemic and cosmopolitan  
1060 diatom-dominated phytoplankton assemblages. *Ecological Indicators* **85**: 878–886.  
1061 doi:10.1016/j.ecolind.2017.11.052
- 1062 Sitnikova, T. Ya. 2012. Определитель брюхоногих моллюсков бухты Большие Коты (юго-  
1063 западное побережье озера Байкал) [Key of the Gastropod Molluscs in the Bay of  
1064 Bolshie Koty (South-West shoreline of Lake Baikal)], Irkutsk State University.
- 1065 Slowikowski, K. 2019. ggrepel: Automatically Position Non-Overlapping Text Labels with  
1066 “ggplot2.”
- 1067 Smith, V. H., G. D. Tilman, and J. C. Nekola. 1999. Eutrophication: impacts of excess nutrient  
1068 inputs on freshwater, marine, and terrestrial ecosystems. *Environmental Pollution* **100**:  
1069 179–196. doi:10.1016/S0269-7491(99)00091-3
- 1070 Sneath, P. H. A., and R. R. Sokal. 1973. *Numerical Taxonomy: The Principles and Practice of*  
1071 *Numerical Classification*, W. H. Freeman.
- 1072 Steinmetz, Z., C. Wollmann, M. Schaefer, and others. 2016. Plastic mulching in agriculture.  
1073 Trading short-term agronomic benefits for long-term soil degradation? *Science of The*  
1074 *Total Environment* **550**: 690–705. doi:10.1016/j.scitotenv.2016.01.153
- 1075 Stoddard, J. L., J. Van Sickle, A. T. Herlihy, J. Brahney, S. Paulsen, D. V. Peck, R. Mitchell, and  
1076 A. I. Pollard. 2016. Continental-Scale Increase in Lake and Stream Phosphorus: Are

- 1077 Oligotrophic Systems Disappearing in the United States? Environ. Sci. Technol. **50**:  
1078 3409–3415. doi:10.1021/acs.est.5b05950
- 1079 Sumner, M. D. 2019. *spdplyr*: Data Manipulation Verbs for the Spatial Classes.,
- 1080 Suzuki, R., Y. Terada, and H. Shimodaira. 2019. *pvclust*: Hierarchical Clustering with P-Values  
1081 via Multiscale Bootstrap Resampling.,
- 1082 Swamikannu, X., and K. D. Hoagland. 1989. Effects of Snail Grazing on the Diversity and  
1083 Structure of a Periphyton Community in a Eutrophic Pond. Can. J. Fish. Aquat. Sci. **46**:  
1084 1698–1704. doi:10.1139/f89-215
- 1085 Swann, G. E. A., V. N. Panizzo, S. Piccolroaz, and others. 2020. Changing nutrient cycling in  
1086 Lake Baikal, the world's oldest lake. PNAS **117**: 27211–27217.  
1087 doi:10.1073/pnas.2013181117
- 1088 Taipale, S., U. Strandberg, E. Peltomaa, A. W. E. Galloway, A. Ojala, and M. T. Brett. 2013.  
1089 Fatty acid composition as biomarkers of freshwater microalgae: analysis of 37 strains of  
1090 microalgae in 22 genera and in seven classes. Aquatic Microbial Ecology **71**: 165–178.  
1091 doi:10.3354/ame01671
- 1092 Takhteev, V. V., and D. I. Didorenko. 2015. Fauna and ecology of amphipods of Lake Baikal: A  
1093 Training manual, V.B. Sochava Institute of Geography SB RAS.
- 1094 Timoshkin, O. A., M. V. Moore, N. N. Kulikova, and others. 2018. Groundwater contamination by  
1095 sewage causes benthic algal outbreaks in the littoral zone of Lake Baikal (East Siberia).  
1096 Journal of Great Lakes Research. doi:10.1016/j.jglr.2018.01.008
- 1097 Timoshkin, O. A., D. P. Samsonov, M. Yamamoto, and others. 2016. Rapid ecological change  
1098 in the coastal zone of Lake Baikal (East Siberia): Is the site of the world's greatest  
1099 freshwater biodiversity in danger? Journal of Great Lakes Research **42**: 487–497.  
1100 doi:10.1016/j.jglr.2016.02.011

- 1101 Tong, Y., M. Wang, J. Peñuelas, and others. 2020. Improvement in municipal wastewater  
1102 treatment alters lake nitrogen to phosphorus ratios in populated regions. *Proc Natl Acad  
1103 Sci USA* **117**: 11566–11572. doi:10.1073/pnas.1920759117
- 1104 Tornqvist, R., J. Jarsjo, J. Pietron, A. Bring, P. Rogberg, S. M. Asokan, and G. Destouni. 2014.  
1105 Evolution of the hydro-climate system in the Lake Baikal basin. *Journal of Hydrology*  
1106 **519**: 1953–1962. doi:10.1016/j.jhydrol.2014.09.074
- 1107 Turetsky, M. R., R. K. Wieder, C. J. Williams, and D. H. Vitt. 2000. Organic matter accumulation,  
1108 peat chemistry, and permafrost melting in peatlands of boreal Alberta. *Écoscience* **7**:  
1109 115–122. doi:10.1080/11956860.2000.11682608
- 1110 Veloza, A. J., F.-L. E. Chu, and K. W. Tang. 2006. Trophic modification of essential fatty acids  
1111 by heterotrophic protists and its effects on the fatty acid composition of the copepod  
1112 *Acartia tonsa*. *Marine Biology* **148**: 779–788. doi:10.1007/s00227-005-0123-1
- 1113 Volkova, E. A., N. A. Bondarenko, and O. A. Timoshkin. 2018. Morphotaxonomy, distribution  
1114 and abundance of *Spirogyra* (Zygnematophyceae, Charophyta) in Lake Baikal, East  
1115 Siberia. *Phycologia* **57**: 298–308. doi:10.2216/17-69.1
- 1116 de Vries, J. 1972. Soil Filtration of Wastewater Effluent and the Mechanism of Pore Clogging.  
1117 *Journal (Water Pollution Control Federation)* **44**: 565–573.
- 1118 Wang, W., and J. Wang. 2018. Investigation of microplastics in aquatic environments: An  
1119 overview of the methods used, from field sampling to laboratory analysis. *TrAC Trends  
1120 in Analytical Chemistry* **108**: 195–202. doi:10.1016/j.trac.2018.08.026
- 1121 Wayland, M., and K. A. Hobson. 2001. Stable carbon, nitrogen, and sulfur isotope ratios in  
1122 riparian food webs on rivers receiving sewage and pulp-mill effluents. *Can. J. Zool.* **79**:  
1123 5–15. doi:10.1139/z00-169
- 1124 Wickham, H., M. Averick, J. Bryan, and others. 2019. Welcome to the tidyverse. *Journal of  
1125 Open Source Software* **4**: 1686. doi:10.21105/joss.01686
- 1126 Wilke, C. O. 2019. cowplot: Streamlined Plot Theme and Plot Annotations for “ggplot2.”

- 1127 Wilke, C. O. 2020. *ggtext*: Improved Text Rendering Support for “*ggplot2*,.”
- 1128 Yang, Y., W. Song, H. Lin, W. Wang, L. Du, and W. Xing. 2018. Antibiotics and antibiotic  
1129 resistance genes in global lakes: A review and meta-analysis. *Environment International*  
1130 **116**: 60–73. doi:10.1016/j.envint.2018.04.011
- 1131 Yang, Y.-Y., G. S. Toor, P. C. Wilson, and C. F. Williams. 2016. Septic systems as hot-spots of  
1132 pollutants in the environment: Fate and mass balance of micropollutants in septic  
1133 drainfields. *Science of The Total Environment* **566–567**: 1535–1544.  
1134 doi:10.1016/j.scitotenv.2016.06.043
- 1135 York, J. K., G. Tomasky, I. Valiela, and D. J. Repeta. 2007. Stable isotopic detection of  
1136 ammonium and nitrate assimilation by phytoplankton in the Waquoit Bay estuarine  
1137 system. *Limnology and Oceanography* **52**: 144–155. doi:10.4319/lo.2007.52.1.0144
- 1138 Yoshida, T., T. Sekino, M. Genkai-Kato, and others. 2003. Seasonal dynamics of primary  
1139 production in the pelagic zone of southern Lake Baikal. *Limnology* **4**: 53–62.  
1140 doi:10.1007/s10201-002-0089-3
- 1141 Yoshii, K. 1999. Stable isotope analyses of benthic organisms in Lake Baikal. *Hydrobiologia*  
1142 **411**: 145–159.
- 1143 2016a. Methods for determination of nitrogen-containing matters (with corrections) (Методы  
1144 определения азотсодержащих веществ (с Поправками)).
- 1145 2016b. Methods for determination of phosphorus-containing matters (with corrections) (Методы  
1146 определения фосфорсодержащих веществ).
- 1147 2017. Nitrate concentration in waters: Photometric methods with Giress reagent following  
1148 stabilization in a cadmium reducer (Массовая концентрация нитратного азота в  
1149 водах: Методика измерений фотометрическим методом с реагентом Грисса после  
1150 восстановления в камиевом редукторе).
- 1151

1152 **Acknowledgments**

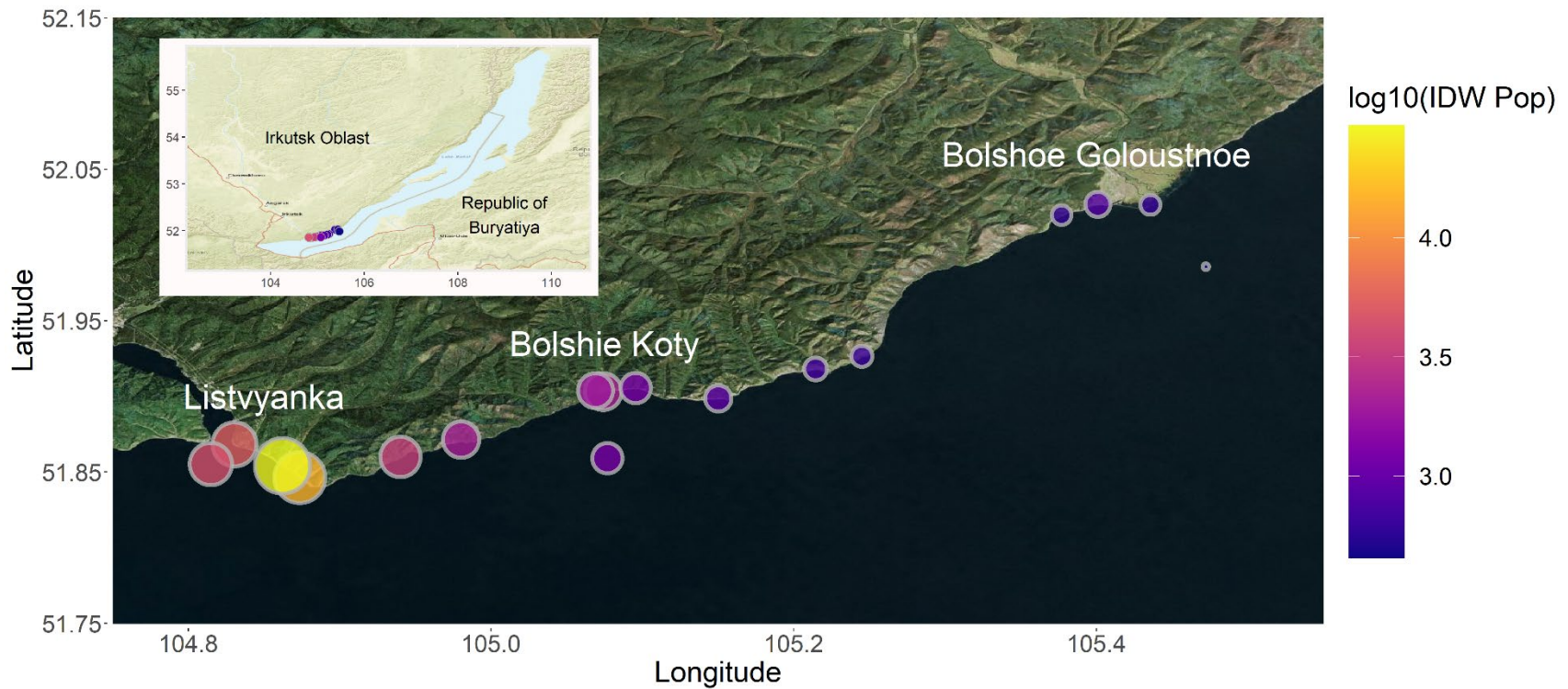
1153

1154 We would like to thank the faculty, students, staff, and mariners of the Irkutsk State University's  
1155 Biological Research Institute Biostation for their expert field, taxonomic, and laboratory support;  
1156 Marianne Moore and Bart De Stasio for helpful advice; the researchers and students of the  
1157 Siberian Branch of the Russian Academy of Sciences Limnological Institute for expert  
1158 taxonomic and logistical assistance; Oleg A. Timoshkin, Tatiana Ya. Sitnikova, Irina V.  
1159 Mekhanikova, Nina A. Bonderenko, Ekaterina Volkova, Yulia Zvereva, Vadim V. Takhteev,  
1160 Stephanie G. Labou, Stephen L. Katz, Brian P. Lanouette, John R. Loffredo, Alli N. Cramer,  
1161 Alexander K. Fremier, Erica J. Crespi, Stephen M. Powers, Daniel L. Preston, Gavin L.  
1162 Simpson, and James J. Elser for offering insights throughout the development of this project.  
1163 Funding was provided by the National Science Foundation (NSF-DEB-1136637) to S.E.H., a  
1164 Fulbright Fellowship to M.F.M., a NSF Graduate Research Fellowship to M.F.M. (NSF-DGE-  
1165 1347973), and the Russian Ministry of Education and Science Research Project (No. GR  
1166 01201461929; 1354-2014/51). This work serves as one chapter of M.F.M.'s doctoral dissertation  
1167 in Environmental and Natural Resource Sciences at Washington State University.

1168

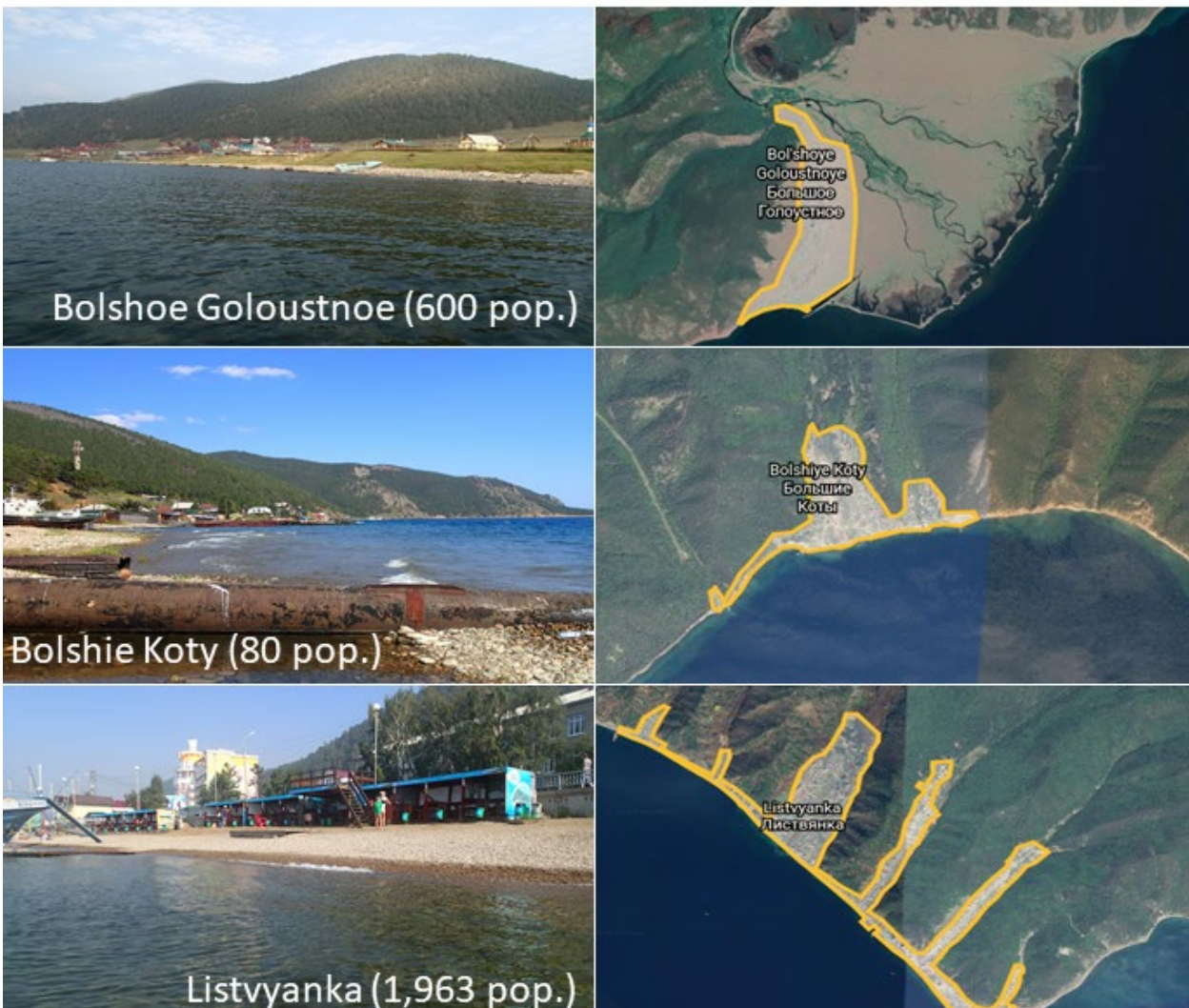
Table 1: Location, depth, temperature and population information for each of the 17 sampling stations. “OS” refers to pelagic locations (i.e., “Offshore”), whereas other site abbreviations refer to littoral sampling locations.

Site	Latitude	Longitude	Depth (m)	Distance to shore (m)	Air Temperature (°C)	Surface Temperature (°C)	Adjacent Population
BK-1	51.90316	105.07404	0.7	10	18	14	80
BK-2	51.90365	105.069	0.9	17.5	19	13	80
BK-3	51.90536	105.0957	0.8	10	18	14	80
BGO-1	52.02693	105.40102	0.9	18	20	13	0
BGO-2	52.0197	105.37707	1.1	14	19	14	600
BGO-3	52.02649	105.43577	0.7	21	18	16	600
OS-1	51.98559	105.47237	900	NA	15	NA	NA
KD-1	51.92646	105.24504	0.8	20.75	23	NA	0
KD-2	51.91807	105.21456	0.9	14.5	23	16	0
MS-1	51.89863	105.15017	0.6	10.5	21	17	0
SM-1	51.87152	104.98006	0.9	11.5	21	15	0
LI-1	51.86825	104.83042	0.6	8.9	19	14	2000
LI-2	51.84626	104.87356	0.8	9.4	21	15	2000
LI-3	51.85407	104.86216	0.7	9.25	19.5	15	2000
EM-1	51.86005	104.93999	0.7	15.5	24.5	14	0
OS-2	51.8553	104.8148	1300	NA	21	NA	NA
OS-3	51.859108	105.0769	1400	5000	NA	14.5	NA



1171  
 1172 Figure 1: Map of all sampling locations with sites sized and colored by log-transformed IDW population. IDW population was log-  
 1173 transformed so as to make IDW populations across three orders of magnitude more comparable. The entire transect included three  
 1174 developed sites (i.e., Listvyanka, Bolshie Koty, Bolshoe Goloustnoe). Three offshore samples were also collected to compare pelagic  
 1175 sewage signals to those in the littoral. Sampling locations west of Listvyanka are located farther from Listvyanka's centroid, and  
 1176 therefore have lower IDW population values than sites located closer to the centroid. This map was created using the R statistical  
 1177 environment (R Core Team 2019) and the tidyverse (Wickham et al. 2019), OpenStreetMap (Fellows and Stotz 2019), ggrepel  
 1178 (Kassambara 2019), cowplot (Wilke 2019), and ggrepel (Slowikowski 2019) packages.  
 1179

1180

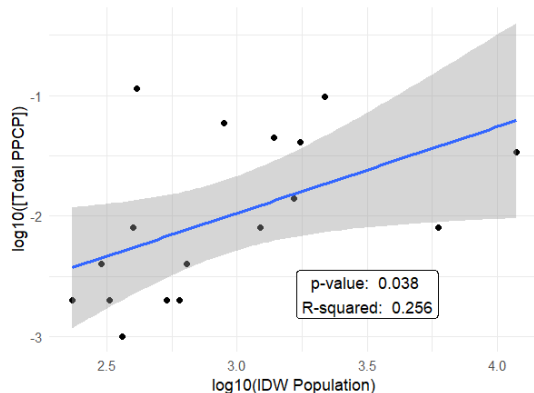
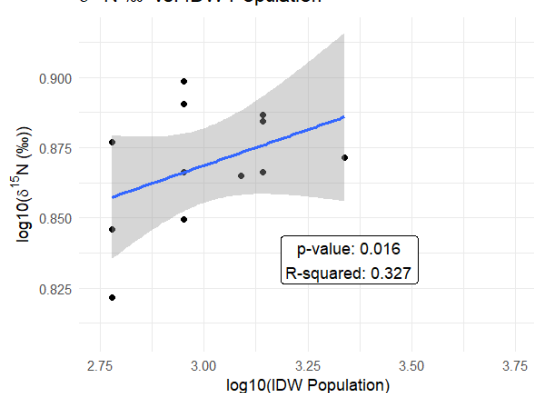
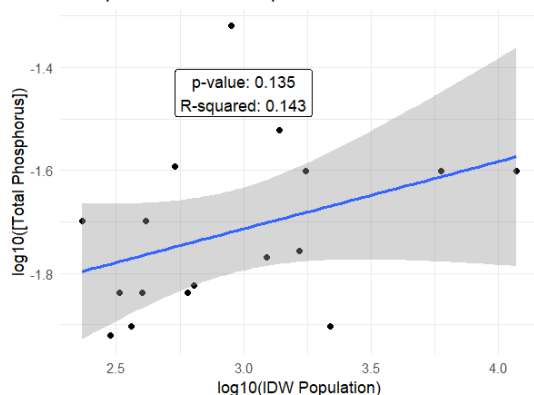
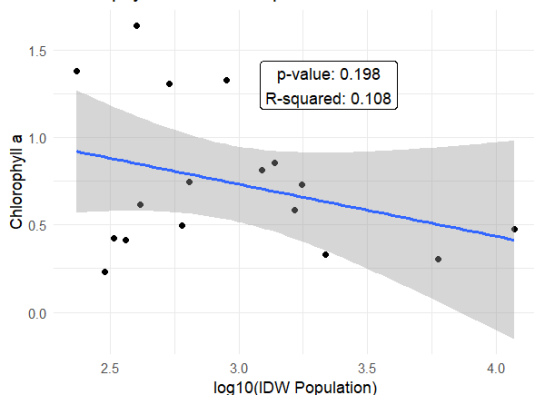
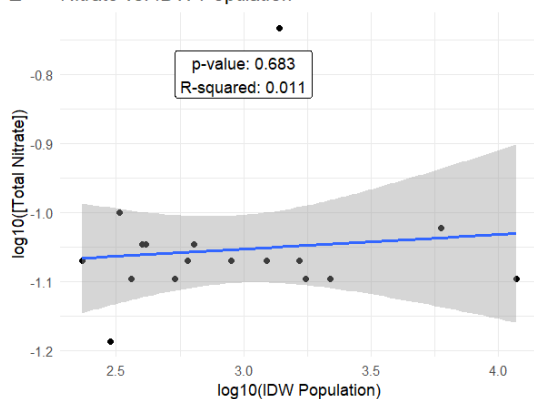
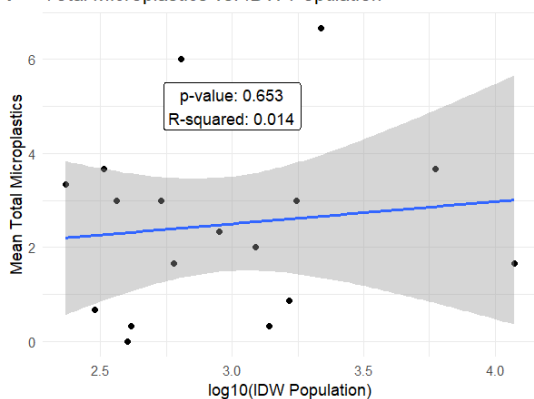
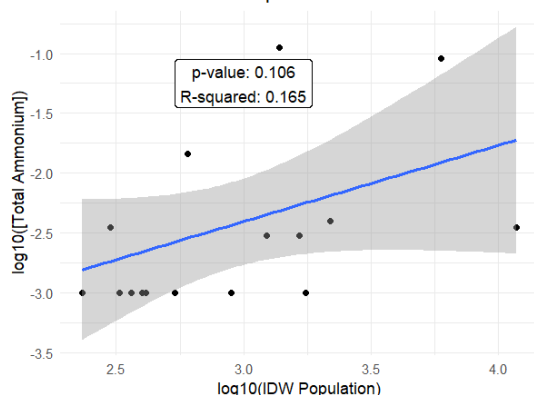
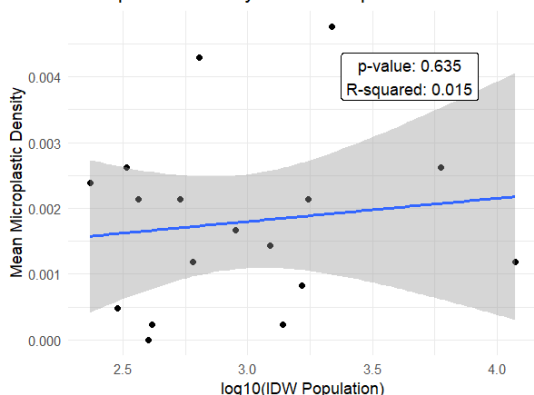


1181

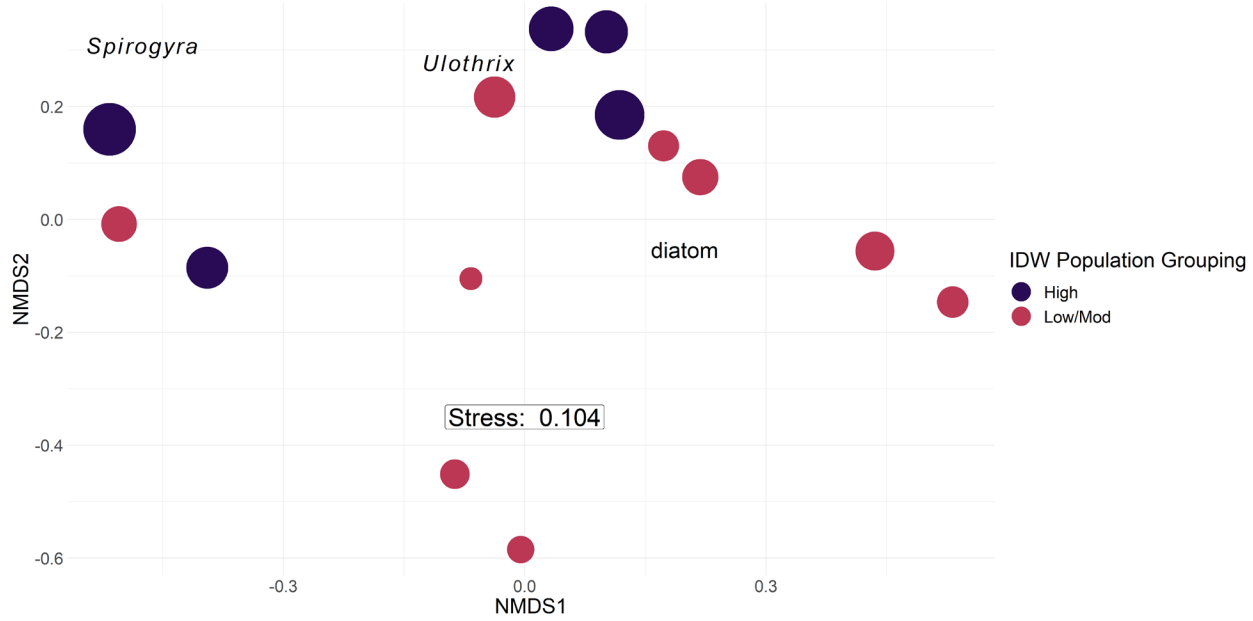
1182 Figure 2: Photographs and Google Earth imagery of each developed area. Photographs were  
1183 taken by Kara H. Woo and Michael F. Meyer.

Table 2: Average sewage indicator concentrations and densities per sampling location. Caffeine, acetaminophen/paracetamol, paraxanthine, and cotinine detection limits are estimated to be 0.001 µg/L based on a 500 mL sample volume.

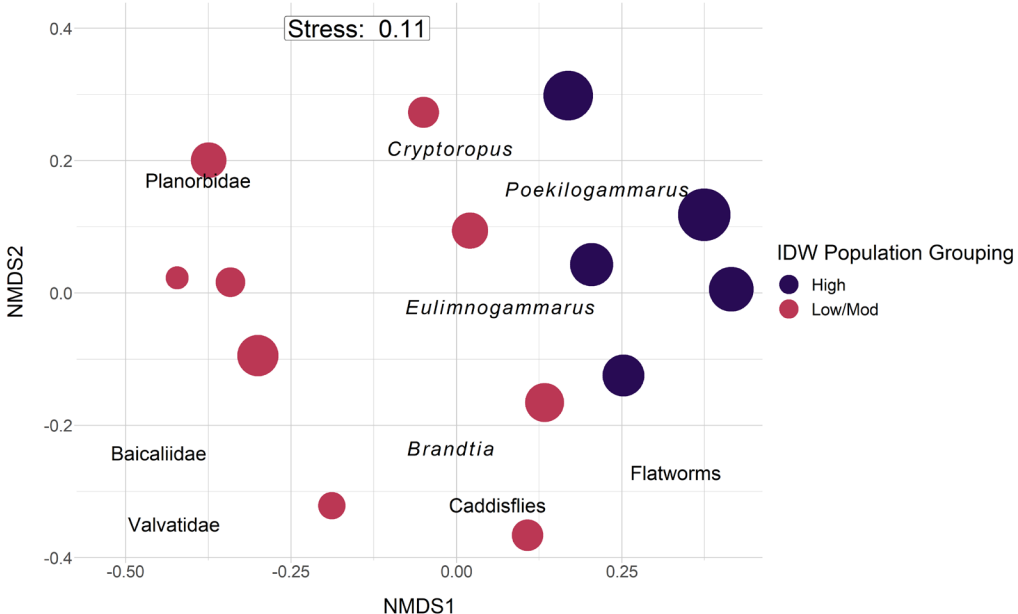
Site	NH <sub>4</sub> <sup>+</sup> (mg/L)	NO <sub>3</sub> <sup>-</sup> (mg/L)	Total Phosphorus (mg/L)	Caffeine (µg/L)	Acetaminophen (µg/L)	Paraxanthine (µg/L)	Cotinine (µg/L)	Fragment density (MPs/L)	Fiber density (MPs/L)	Bead density (MPs/L)	IDW population	Categorical IDW population
BK-1	0.003	0.085	0.054	0.011	0.001	0.002	0	0	0.000833	0	2304.039	High
BK-2	0.003	0.085	0.052	0.007	0.001	0	0	0.000952	0.000476	0	1891.558	Mod/Low
BK-3	0.068	0.09	0.045	0.003	0.001	0	0	0.003095	0.00119	0	1231.234	Mod/Low
BGO-1	0.0145	0.085	0.044	0	0.002	0	0	0.00119	0	0	838.5385	Mod/Low
BGO-2	0.001	0.08	0.0385	0	0.001	0	0	0.000238	0.001905	0	611.91	Mod/Low
BGO-3	0.001	0.09	0.044	0.005	0.003	0	0	0	0	0	624.455	Mod/Low
OS-1	0.001	0.085	0.061	0	0.001	0	0.001	0.002381	0	0	455.7733	Mod/Low
KD-1	0.0035	0.065	0.0375	0.003	0.001	0	0	0	0.000476	0	662.4151	Mod/Low
KD-2	0.001	0.1	0.0445	0.001	0.001	0	0	0.000714	0.001905	0	720.5484	Mod/Low
MS-1	0.001	0.09	0.061	0.064	0.035	0.015	0	0	0.000238	0	903.6733	Mod/Low
SM-1	0.001	0.085	0.1475	0.042	0.012	0.005	0	0	0.001667	0	2146.218	Mod/Low
LI-1	0.004	0.08	0.0385	0.05	0.04	0.006	0.002	0.00381	0.000238	0.000714	5403.209	High
LI-2	0.091	0.095	0.0775	0.001	0.007	0	0	0.001429	0.00119	0	14792.51	High
LI-3	0.0035	0.08	0.077	0.027	0.002	0.002	0.003	0.000476	0	0.000714	29511.73	High
EM-1	0.1125	0.185	0.092	0.029	0.014	0.002	0	0	0.000238	0	3389.949	High
OS-2	0.001	0.08	0.078	0.033	0.001	0.004	0.003	0.000238	0.001905	0	4340	High
OS-3	0.001	0.08	0.0795	0.001	0.001	0	0	0	0.002143	0	1221.424	Mod/Low

**A** PPCP vs. IDW Population**B**  $\delta^{15}\text{N } \text{\%}$  vs. IDW Population**C** Phosphorus vs. IDW Population**D** Chlorophyll a vs. IDW Population**E** Nitrate vs. IDW Population**F** Total Microplastics vs. IDW Population**G** Ammonium vs. IDW Population**H** Microplastics Density vs. IDW Population

1186 Figure 3: Linear models of total PPCP concentrations (A), macroinvertebrate  $\delta^{15}\text{N}$  (B), total  
1187 phosphorus (C), chlorophyll a (D), nitrate (E), total microplastics (F), ammonium (G), and  
1188 microplastic density (H) regressed against log-transformed inverse distance weighted (IDW)  
1189 population. Total PPCP concentrations (A) and macroinvertebrate  $\delta^{15}\text{N}$  (B) produced significant  
1190 models. Total phosphorus (C), chlorophyll a (D), nitrate (E), total microplastics (F), ammonium  
1191 (G), and microplastic density (H) did not produce significant models.

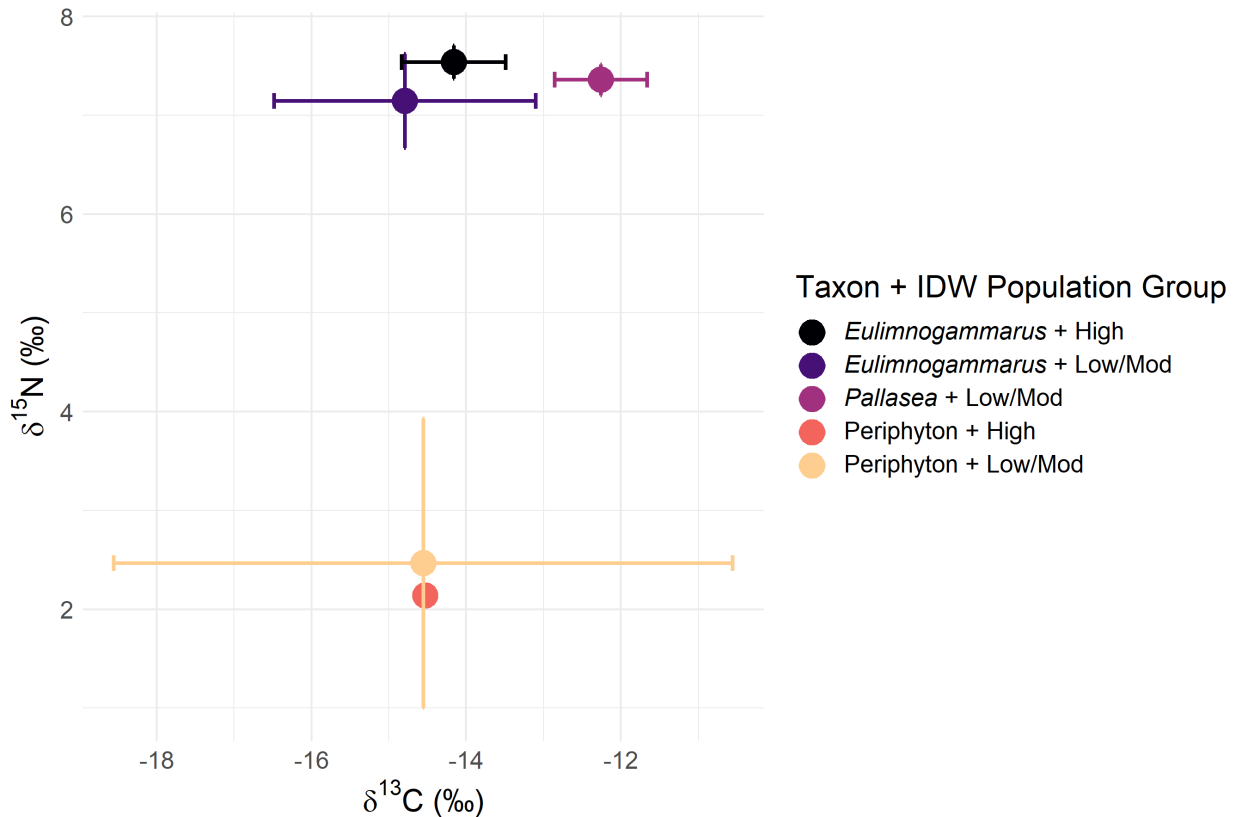


1192  
1193 Figure 4: Periphyton abundance NMDS with Bray-Curtis dissimilarity. Points are sized by log10  
1194 IDW population and colored by grouped IDW population values. Taxonomic labels represent  
1195 species scores, which are weighted averages of species contributions from site scores. For  
1196 periphyton, PERMANOVA ( $p = 0.001$ ) and post-hoc SIMPER results suggested sites with a  
1197 higher IDW population value tended to be more associated with filamentous algal groupings and  
1198 separate from sites with moderate and low IDW population values, which were more associated  
1199 with diatom abundance.  
1200



1201  
1202  
1203  
1204  
1205  
1206  
1207  
1208  
1209

Figure 5: Macroinvertebrate abundance NMDS with Bray-Curtis dissimilarity. Points are sized by log10 IDW population and colored by grouped IDW population values. Taxonomic labels represent species scores, which are weighted averages of species contributions from site scores. For macroinvertebrates, PERMANOVA ( $p = 0.02$ ) and post-hoc SIMPER results suggested sites with a higher IDW population values tended to be associated with amphipod taxa (see Table S1), whereas sites with lower and moderate IDW population values were more associated with increased mollusk abundance (see Table S1).

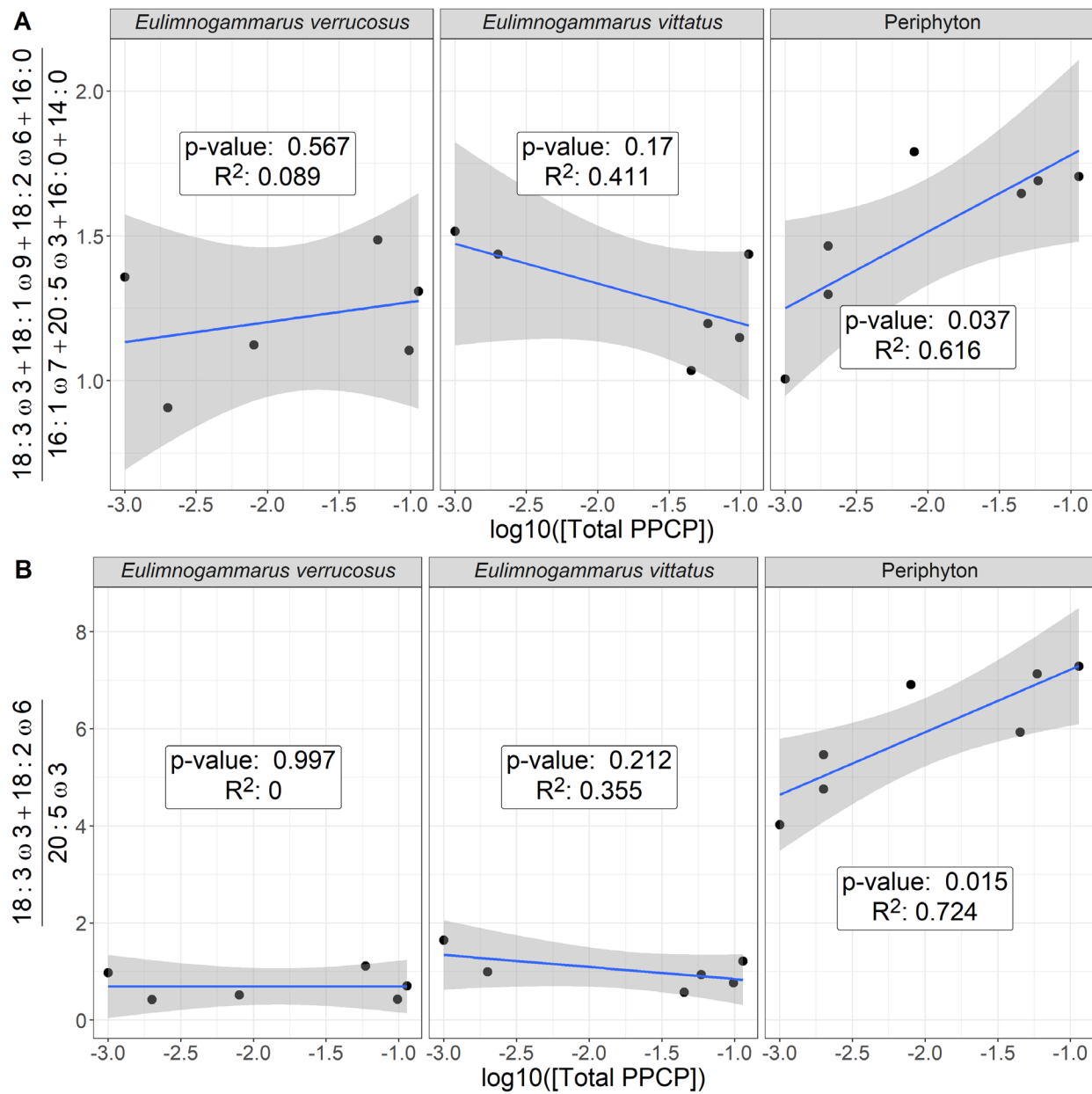


1210  
1211  
1212  
1213  
1214  
1215  
1216  
1217  
1218  
1219

Figure 6: Biplot of mean and standard deviation  $\delta^{13}\text{C}$  and  $\delta^{15}\text{N}$  stable isotope values for littoral amphipods and periphyton, grouped by categorical IDW population (Table 3). In general, periphyton did not differ in  $\delta^{13}\text{C}$  or  $\delta^{15}\text{N}$  signatures with increasing IDW population, whereas *Eulimnogammarus* amphipods increased in  $\delta^{15}\text{N}$  signatures with increasing IDW population. *Pallasea* signatures differed from *Eulimnogammarus* most likely because *Pallasea* tends to remain in the nearshore area, whereas *Eulimnogammarus* will regularly migrate to deeper zones (Takhteev & Didorenko, 2015).

Table 3: Mean inter-site fatty acid proportion of each taxon and fatty acid grouping (as defined in table S2).

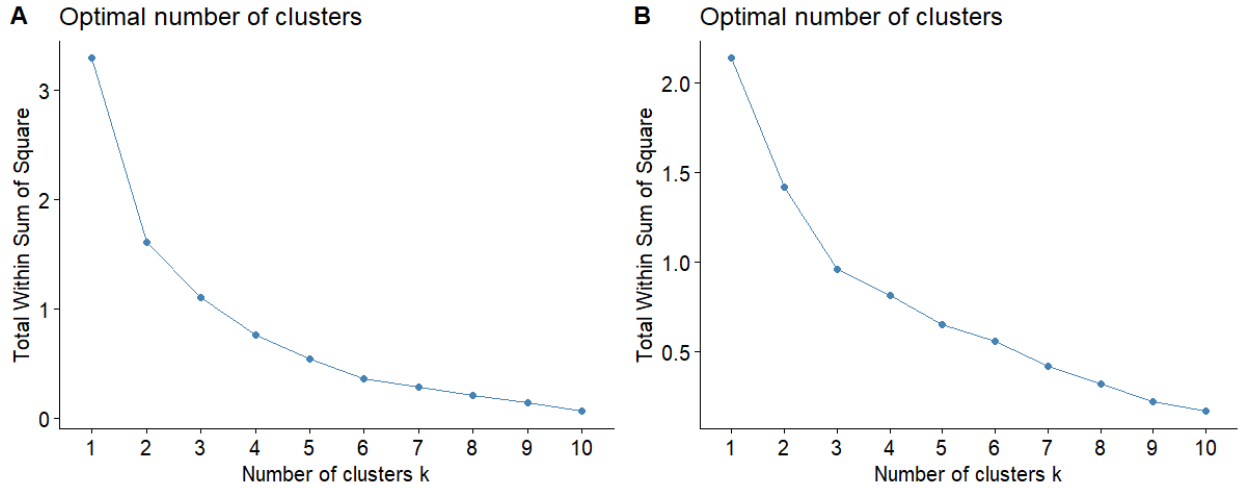
<b>Taxon</b>	<b>Number of sites</b>	<b>Branched</b>	<b>LCPUFA</b>	<b>MUFA</b>	<b>SAFA</b>	<b>SCPUFA</b>
<i>Draparnaldia</i> spp.	4	0.000	0.012	0.088	0.189	0.710
<i>Eulimnogammarus cyaneus</i>	2	0.002	0.259	0.309	0.248	0.182
<i>Eulimnogammarus verrucosus</i>	6	0.000	0.188	0.385	0.240	0.187
<i>Eulimnogammarus vittatus</i>	6	0.001	0.171	0.371	0.241	0.216
<i>Pallasea cancellus</i>	3	0.001	0.282	0.359	0.187	0.171
Periphyton	7	0.000	0.073	0.092	0.284	0.550
Snail	3	0.002	0.470	0.123	0.194	0.211



1223 Figure 7: Ratio of filamentous:diatom-associated fatty acids (A) and essential fatty acids (B)  
1224 across our PPCP gradient. Our first analysis (A) focused solely on green filamentous algal fatty  
1225 acids (i.e., 18:3ω3, 18:1ω9, 18:2ω6, and 16:0 relative to diatom fatty acids (i.e., 20:5ω3, 16:1ω7,  
1226 16:0, 14:0) in relation to increasing PPCP concentrations. This first analysis suggested  
1227 periphyton reflected an increasing green, filamentous signature relative to diatoms, which  
1228 corroborates analyses showing community compositional shifts (Figure 4). While periphyton  
1229 fatty acids changed significantly across our sewage gradient, macroinvertebrate signatures  
1230 remained consistent. Our second analysis (B) focused solely on the essential fatty acids, which  
1231 further highlights the trends observed in periphyton and macroinvertebrate grazers.

Table S1: Macroinvertebrate taxonomic groupings for abundance estimates. Amphipod taxa were defined as in Takhteev & Didorenko, 2015; mollusk taxa were defined as in Sitnikova, 2012.

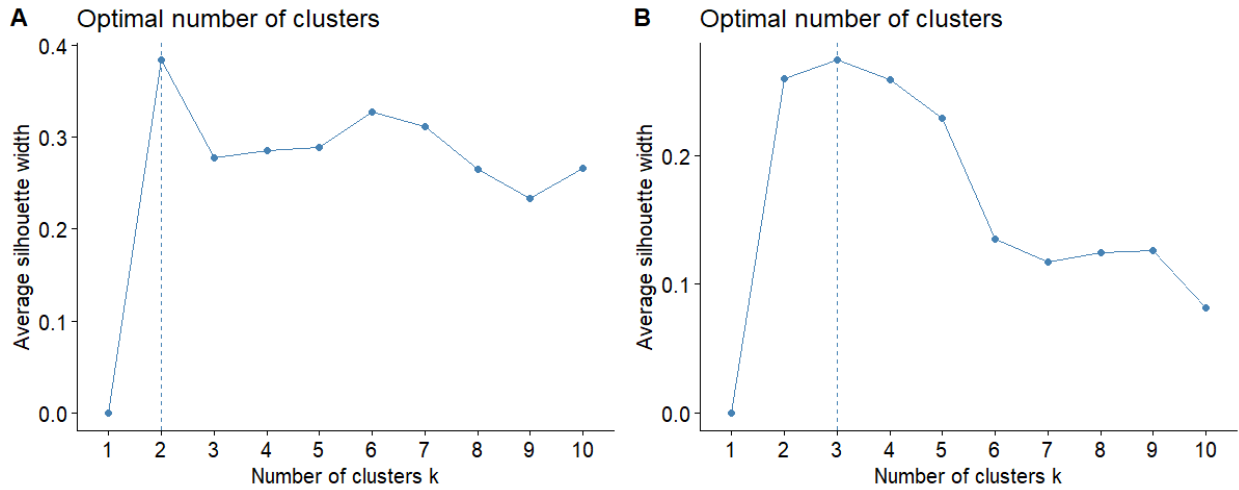
Amphipoda	Mollusca	Other
<i>Brandtia latissima intermida</i> (Dorogostaiskii 1930)	Acroloxiidae	Asellidae
<i>Brandtia latissima lata</i> (Dybowsky 1874)	Baicaliidae	Caddisflies
<i>Brandtia latissima latior</i> (Dybowsky 1874)	Benedictidate	Hirudinea
<i>Brandtia latissima latissima</i> (Gerstfeldt 1858)	Maackia	Planaria
<i>Brandtia parasitica parasitica</i> (Dybowsky 1874)	Planorbidae	
<i>Cryptoropush inflatus</i> (Dybowsky 1874)	Valvatidae	
<i>Cryptoropush pachytus</i> (Dybowsky 1874)		
<i>Cryptoropush rugosus</i> (Dybowsky 1874)		
<i>Eulimnogammarus capreolus</i> (Dybowsky 1874)		
<i>Eulimnogammarus cruentes</i> (Dorogostaiskii 1930)		
<i>Eulimnogammarus cyaneus</i> (Dybowsky 1874)		
<i>Eulimnogammarus grandimanus</i> (Bazikalova 1945)		
<i>Eulimnogammarus maacki</i> (Gerstfeldt 1858)		
<i>Eulimnogammarus maritui</i> (Bazikalova 1945)		
<i>Eulimnogammarus verucossus</i> (Gerstfeldt 1858)		
<i>Eulimnogammarus viridis viridis</i> (Dybowsky 1874)		
<i>Eulimnogammarus vittatus</i> (Dybowsky 1874)		
<i>Pallasea brandtia brandtia</i> (Dybowsky 1874)		
<i>Pallasea brandtii tenera</i> (Sovinskii 1930)		
<i>Pallasea cancelloides</i> (Gerstfeldt 1858)		
<i>Pallasea cancellus</i> (Pallas 1776)		
<i>Pallasea viridis</i> (Garjajev 1901)		
<i>Poekilogammarus crassimus</i> (Sovinskii 1915)		
<i>Poekilogammarus ephippiatus</i> (Dybowsky 1874)		
<i>Poekilogammarus megonychus perpolitus</i> (Takhteev 2002)		
<i>Poekilogammarus pictus</i> (Dybowsky 1874)		



1233  
1234

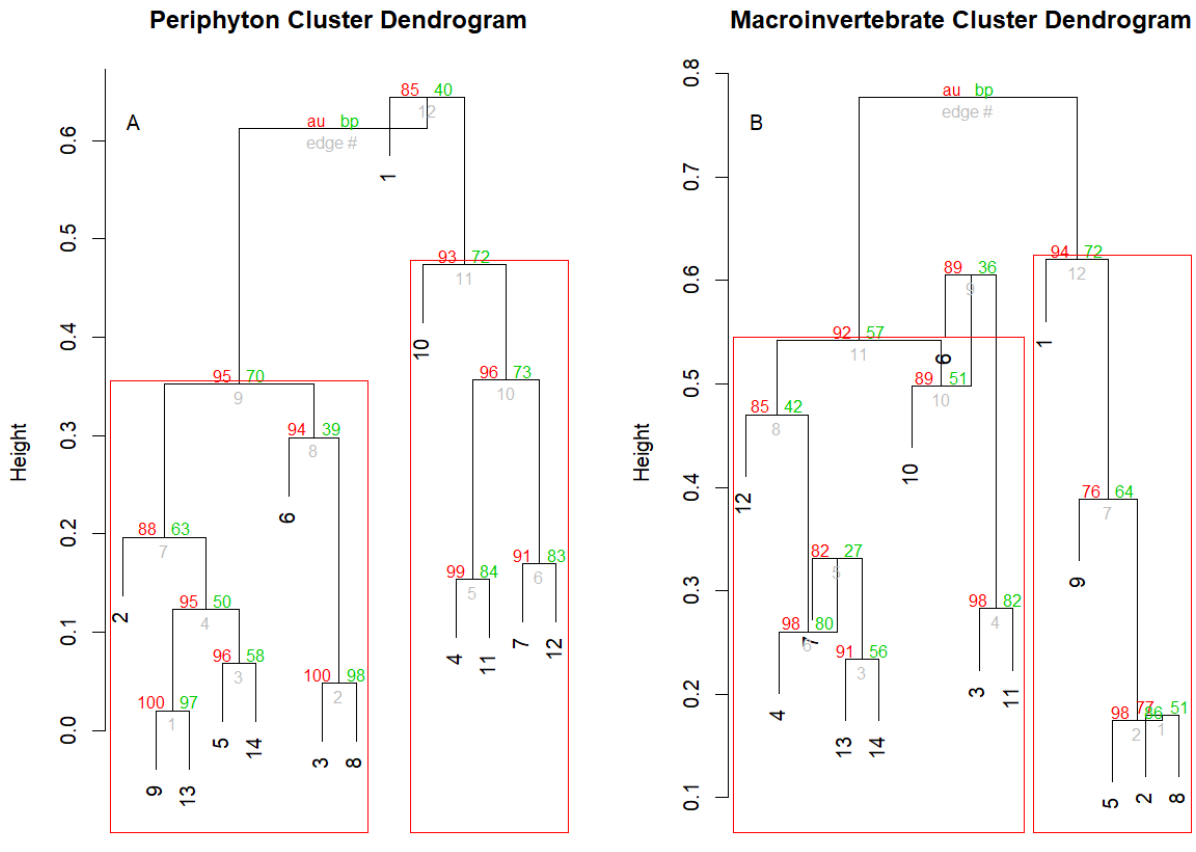
1235 Figure S1: With-group-sum-of-squares (wss) for increasing number of k-mediod clusters for  
1236 periphyton (A) and invertebrate (B) community data. In the case of periphyton data, wss  
1237 decreases most markedly with three clusters, whereas invertebrate community abundance is best  
1238 described by potential two or three clusters.

1239



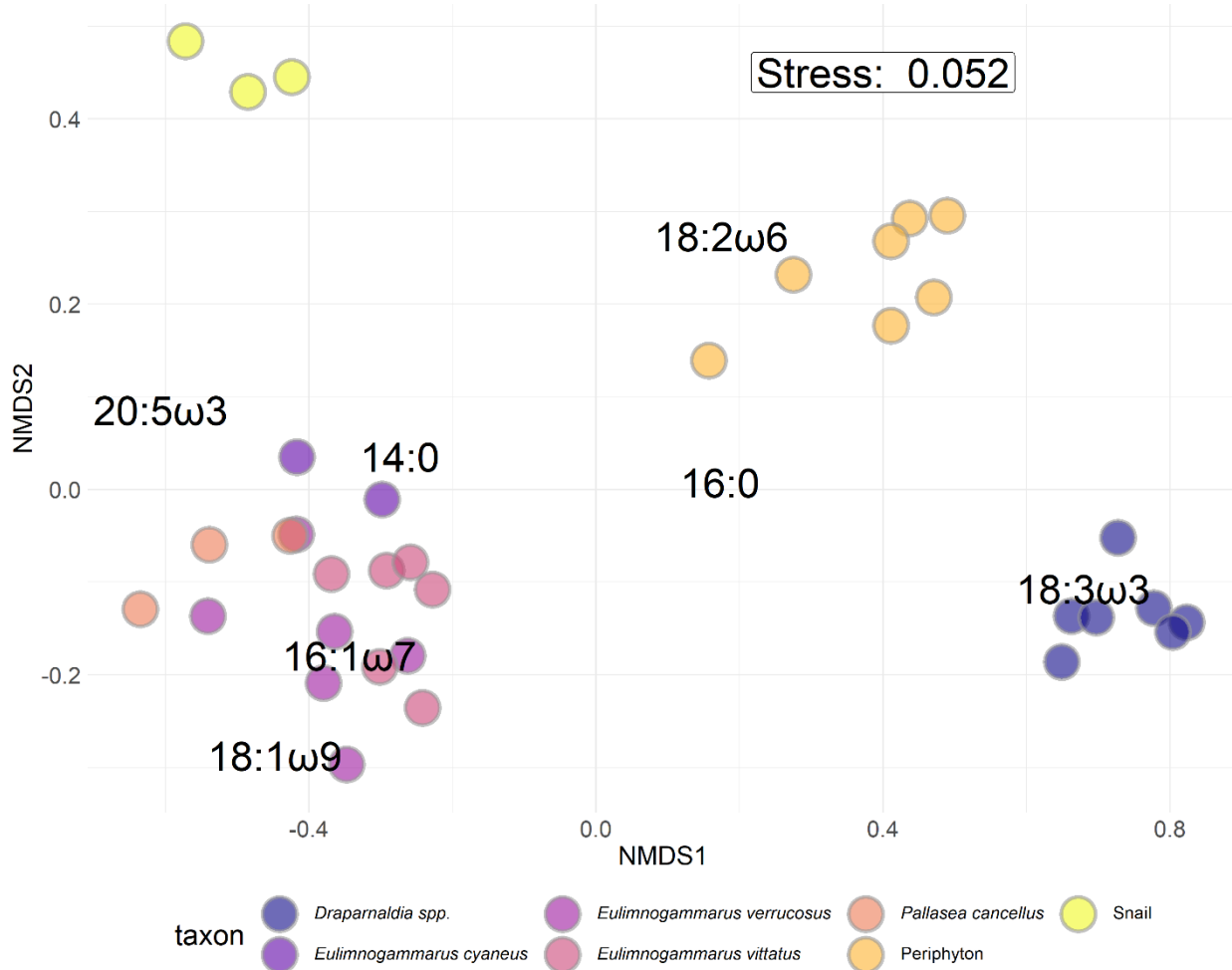
1240  
1241  
1242  
1243  
1244  
1245  
1246

Figure S2: Average silhouette width for increasing number of  $k$ -mediod clusters for periphyton (A) and invertebrate (B) community data. In the case of periphyton data, average silhouette width decreases most markedly with three clusters, whereas invertebrate community abundance is best described by two or three clusters as the average silhouette width for both two and three clusters was highest before beginning to decrease.



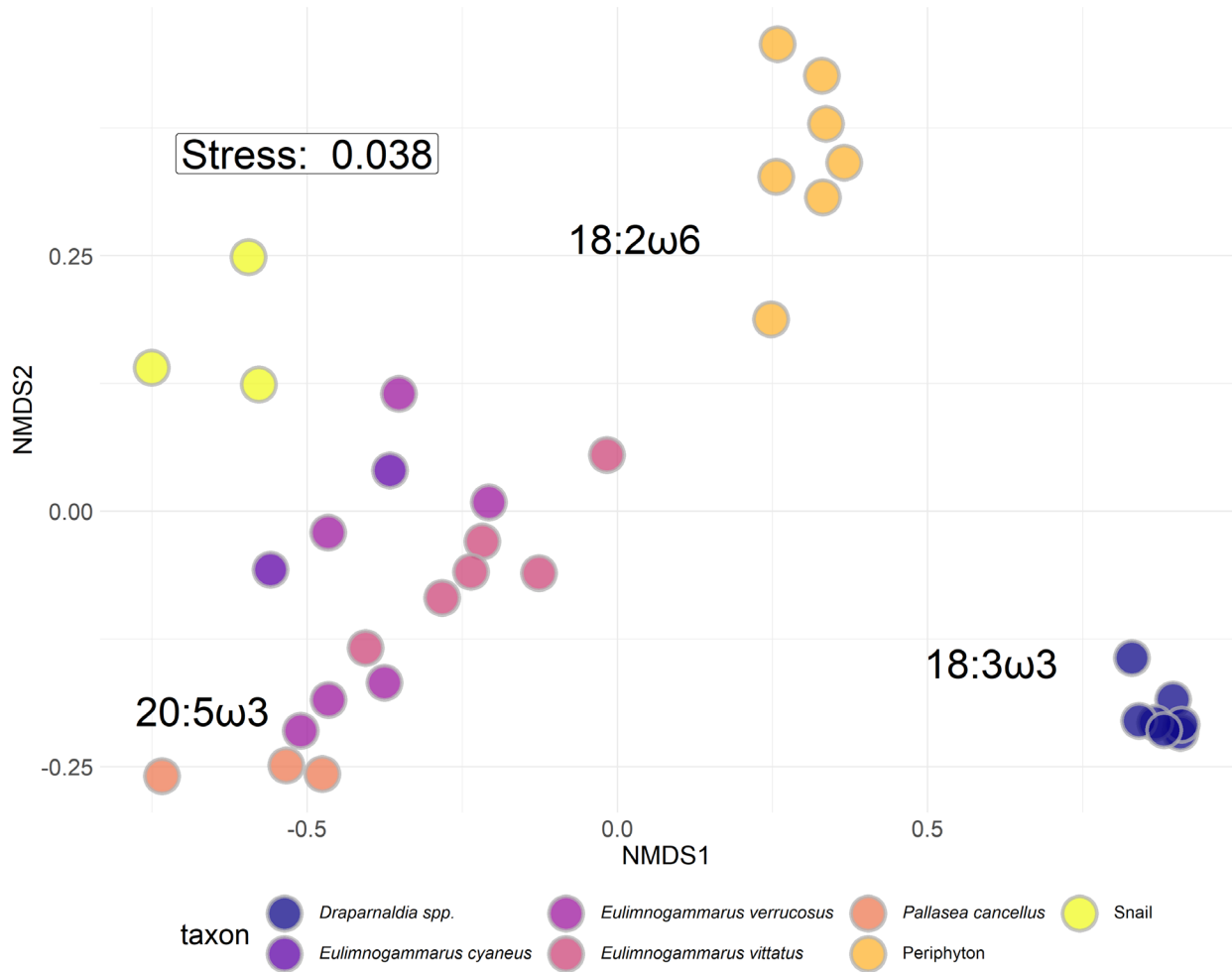
1247  
1248 Figure S3: Weighted Pair-Group Centroid Clustering (WPGMC) for periphyton (A) and  
1249 macroinvertebrate (B) community compositions. Approximately unbiased (au) p-values are  
1250 computed by multiscale bootstrap resampling, and displayed in red on the left side of each node.  
1251 Bootstrapped probabilities (bp) are displayed in green on the right side of each node. Unlike k-  
1252 medioids, WPGMC uses a hierarchical approach to assign clusters, which are bootstrapped in  
1253 order to generate a probability of group membership. This technique suggested that both  
1254 periphyton and macroinvertebrates could be grouped in two clusters. Grouping  
1255 macroinvertebrates into three clusters was possible; however, three clusters resulted in 8 of the  
1256 14 sampling locations being assigned to a group. In contrast, two groups enabled 13 of the 14  
1257 sampling locations to be assigned to a cluster.

### NMDS with Entire FA Spectrum



1258  
1259 Figure S2: NMDS with Bray-Curtis dissimilarity of proportional fatty acid compositions for each  
1260 macroinvertebrate and primary producer collected. *Eulimnogammarus* and *Pallasea* are endemic  
1261 amphipod genera. *Draparnaldia* spp. are endemic filamentous algae that are large and form very  
1262 dense mats easily collected where it occurs. *Draparnaldia* spp. occurred in large, visible  
1263 colonies, allowing us to sample and analyze just the *Draparnaldia* spp. fatty acids. Because  
1264 *Draparnaldia* spp. fatty acids were dominated by 18:3ω3 more so than periphyton, they formed  
1265 their own cluster. Snails were not identified to species prior to fatty acid analysis. Interspecific  
1266 variation in fatty acid composition tended to be larger than intraspecific variation, implying that  
1267 fatty acid signatures were largely species-specific and not environmentally driven.

### NMDS with Essential FA Spectrum



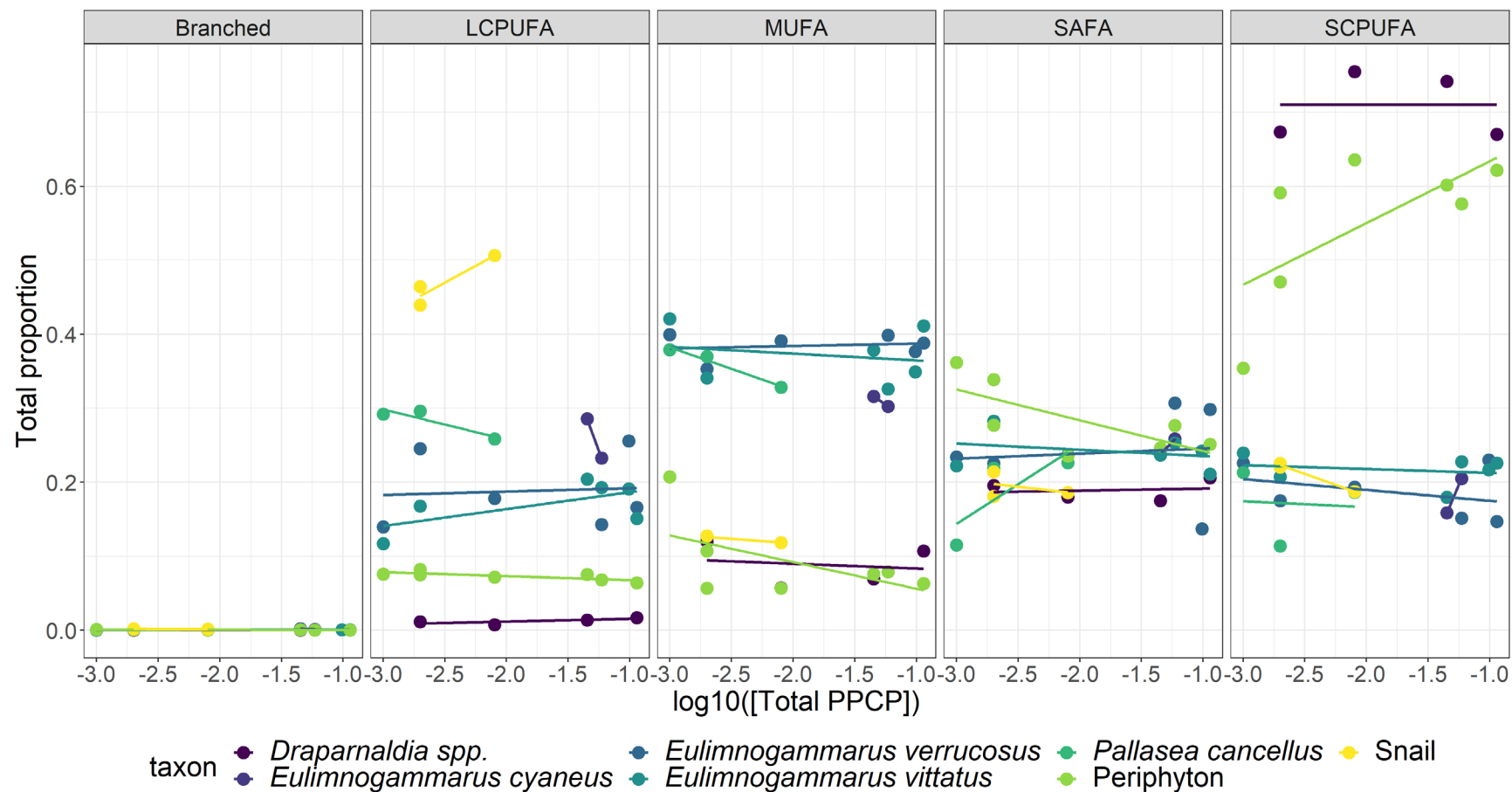
1268  
1269 Figure S3: NMDS with Bray-Curtis dissimilarity of proportional biologically essential fatty acid  
1270 compositions for each macroinvertebrate and primary producer collected. *Eulimnogammarus* and  
1271 *Pallasea* are endemic amphipod genera. *Draparnaldia* spp. are endemic filamentous algae that  
1272 are large and form very dense mats easily collected where it occurs. *Draparnaldia* spp. occurred  
1273 in large, visible colonies, allowing us to sample and analyze just the *Draparnaldia* spp. fatty  
1274 acids. Because *Draparnaldia* spp. fatty acids were dominated by 18:3 $\omega$ 3 more so than  
1275 periphyton, they formed their own cluster. Snails were not identified to species prior to fatty acid  
1276 analysis. Interspecific variation in fatty acid composition tended to be larger than intraspecific  
1277 variation, implying that fatty acid signatures were largely species-specific and not  
1278 environmentally driven.  
1279

Table S2: Fatty acid groupings used in this analysis

Fatty Acid Group	Fatty acids considered
Branched	a-15:0, i-15:0, a-17:0, i-17:0
SAFA	12:0, 14:0, 15:0, 16:0, 17:0, 18:0, 20:0, 22:0, 24:0
MUFA	14:1 $\omega$ 5, 15:1 $\omega$ 7, 17:1n7, 16:1 $\omega$ 5, 16:1 $\omega$ 6, 16:1 $\omega$ 7, 16:1 $\omega$ 8, 16:1 $\omega$ 9, 18:1 $\omega$ 7, 18:1 $\omega$ 9, 20:1 $\omega$ 7, 20:1 $\omega$ 9, 22:1 $\omega$ 7, 22:1 $\omega$ 9
SCPUFA	16:2 $\omega$ 4, 16:2 $\omega$ 6, 16:2 $\omega$ 7, 16:3 $\omega$ 3, 16:3 $\omega$ 4, 16:3 $\omega$ 6, 16:4 $\omega$ 1, 16:4 $\omega$ 3, 18:2 $\omega$ 6, 18:2 $\omega$ 6t, 18:3 $\omega$ 3, 18:3 $\omega$ 6, 18:4 $\omega$ 3, 18:4 $\omega$ 4, 18:5 $\omega$ 3
LCPUFA	20:2 $\omega$ 5(11), 20:2 $\omega$ 5(13), 20:2 $\omega$ 6, 20:3 $\omega$ 3, 20:3 $\omega$ 6, 20:4 $\omega$ 3, 20:4 $\omega$ 6, 20:5 $\omega$ 3, 22:2 $\omega$ 6, 22:3 $\omega$ 3, 22:4 $\omega$ 3, 22:4 $\omega$ 6, 22:5 $\omega$ 3, 22:5 $\omega$ 6, 22:6 $\omega$ 3

1280

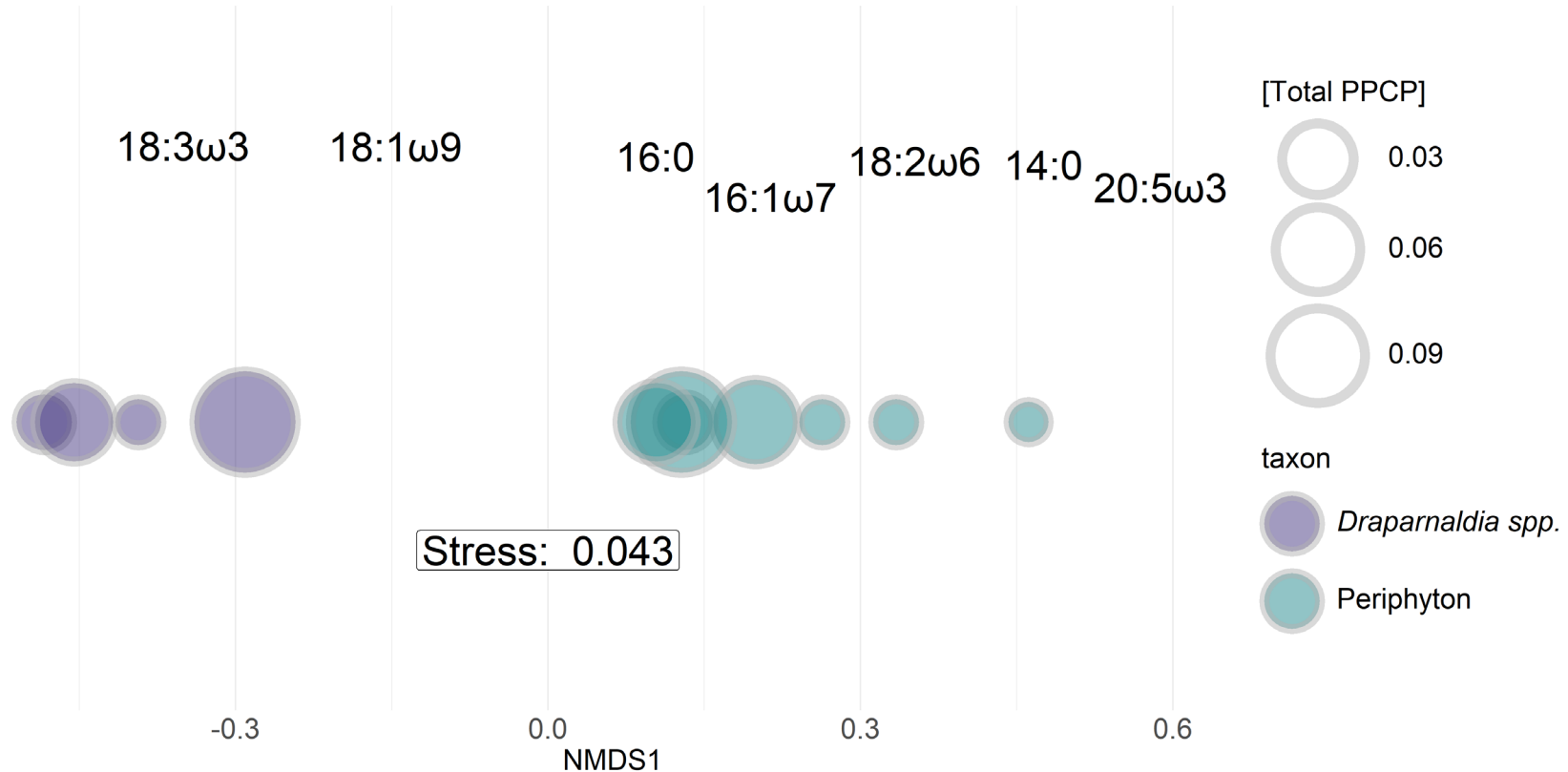
1281



1282  
1283  
1284  
1285  
1286  
1287  
1288  
1289

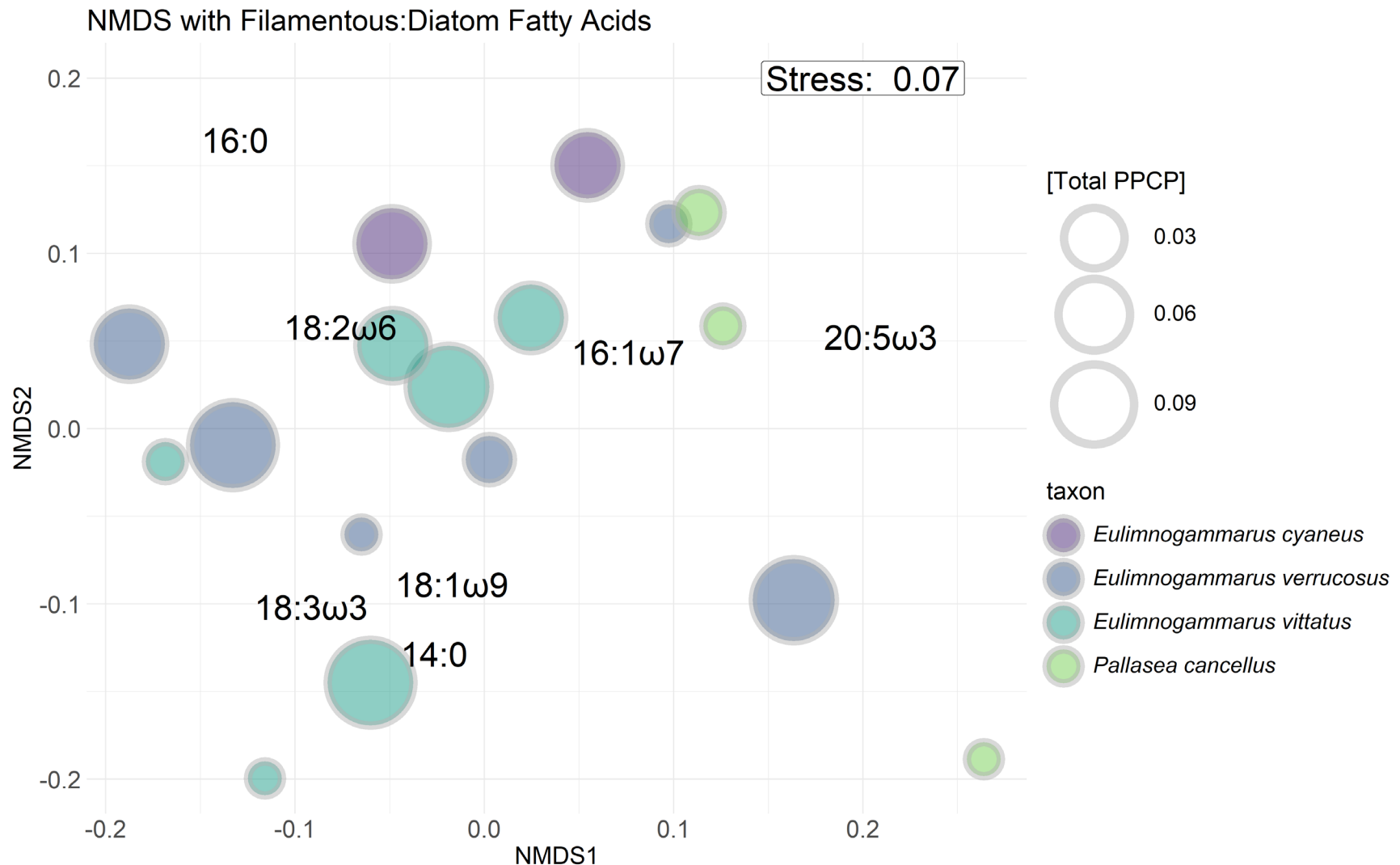
Figure S4: Proportions of major fatty acid groups (as defined in Table S2) across the sewage gradient. Primary producers (*Draparnaldia* spp. and periphyton) were largely characterized by SCPUFAs, amphipods were largely associated with high MUFA abundance, and snails were generally characterized with high LCPUFA abundance. Across the sewage gradient, periphyton SCPUFA tended to increase, which lead to more targeted analyses on which specific fatty acids were increasing. In contrast to periphyton, all other taxa remained consistent with respect to fatty acid proportions across the sewage gradient.

### NMDS with Filamentous:Diatom Fatty Acids



1290  
1291  
1292  
1293  
1294  
1295

Figure S5: One-dimensional NMDS with Bray-Curtis similarity of seven targeted fatty acids of interest for primary producers. Fatty acid scores are placed above shapes. Shapes are sized by total PPCP concentration. Periphyton (blue-green) tend to increase in size from right-to-left, suggesting that periphyton tend to include more 18:3 $\omega$ 3 and 18:1 $\omega$ 9 (indicators of green algal taxa) with an increasing sewage signal. In contrast, *Draparnaldia* spp. (purple) fatty acids tend to remain consistent across the sewage gradient.



1296

1297 Figure S6: NMDS with Bray-Curtis similarity of seven targeted fatty acids of interest for primary producers. Points are sized by total  
 1298 PPCP concentration. Visually, there appears to be no distinct separation among or within taxa unlike was observed with periphyton  
 1299 (Figure S5).

1300